AD-A032 428 BATTELLE COLUMBUS LABS OHIO F/G 11/4
THREE-DIMENSIONAL FINITE ELEMENT STRESS ANALYSIS OF LAMINATED P--ETC(U)
AUG 76 E F RYBICKI, D W SCHMUESER F33615-74-C-5096
UNCLASSIFIED AFML-TR-76-92 NL

1 OF 1
AD A032428

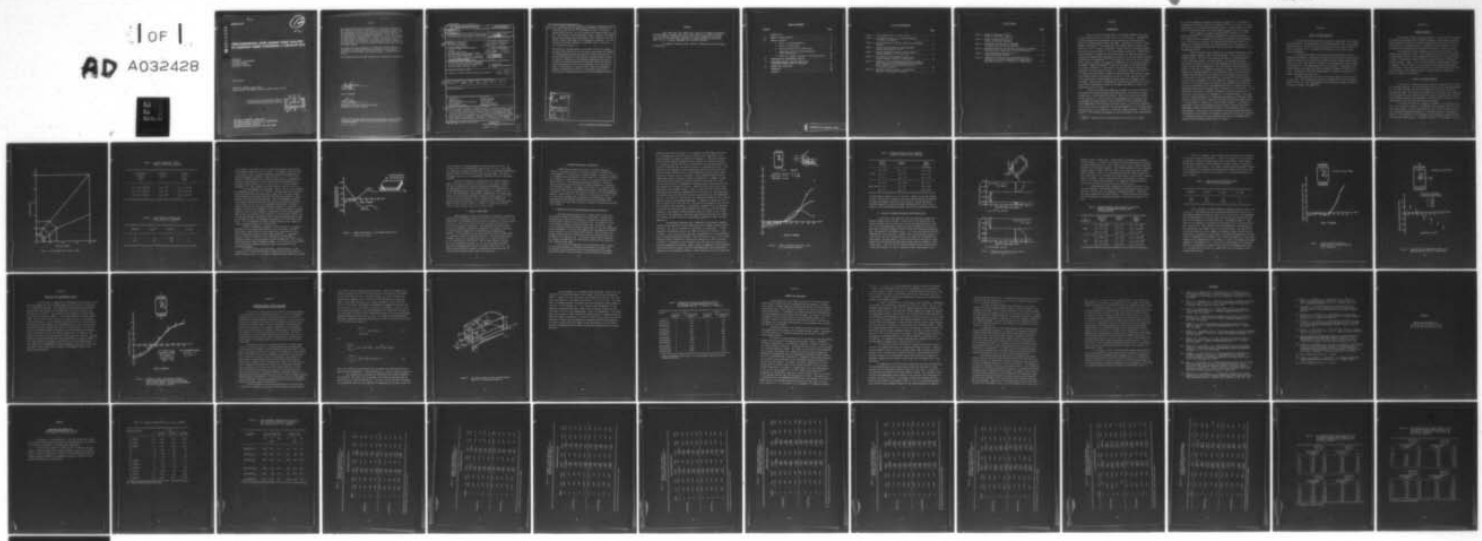

END

DATE FILMED
1-77

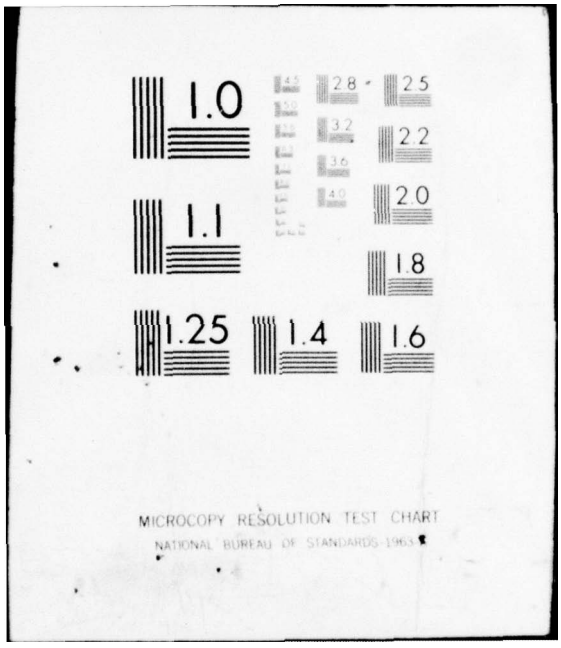
1.0
1.1
1.25
1.4
1.6
1.8
2.0
2.2
2.5
2.8
3.2
3.6
4.0
4.5
MICROCOPY RESOLUTION TEST CHART
NATIONAL BUREAU OF STANDARDS 1963

AFML-TR-76-92

12

NW

THREE-DIMENSIONAL FINITE ELEMENT STRESS ANALYSIS OF LAMINATED PLATES CONTAINING A CIRCULAR HOLE

BATTELLE
COLUMBUS LABORATORIES
505 KING AVENUE
COLUMBUS, OHIO 43201

AUGUST 1976

TECHNICAL REPORT AFML-TR-76-92
FINAL REPORT FOR PERIOD JANUARY 15, 1975 TO JULY 15, 1975

AIR FORCE MATERIALS LABORATORY
AIR FORCE WRIGHT AERONAUTICAL LABORATORIES
AIR FORCE SYSTEMS COMMAND
WRIGHT-PATTERSON AIR FORCE BASE, OHIO 45433

NOTICE

When Government drawings, specifications, or other data are used for any purpose other than in connection with a definitely related Government procurement operation, the United States Government thereby incurs no responsibility nor any obligation whatsoever; and the fact that the Government may have formulated, furnished, or in any way supplied the said drawings, specifications, or other data, is not to be regarded by implication or otherwise as in any manner licensing the holder or any other person or corporation, or conveying any rights or permission to manufacture, use, or sell any patented invention that may be related in any way thereto.

This report has been reviewed by the Information Office (IO) and is releasable to the National Technical Information Service (NTIS). At NTIS, it will be available to the general public, including foreign nations.

This technical report has been reviewed and is approved for publication.

N. J. PAGANO
Project Engineer

FOR THE DIRECTOR

S. W. TSAI, Chief
Mechanics and Surface Interactions Branch
Nonmetallic Materials Division

Copies of this report should not be returned unless return is required by security considerations, contractual obligations, or notice on a specific document.

AIR FORCE - 16 NOVEMBER 76 - 200

UNCLASSIFIED
SECURITY CLASSIFICATION OF THIS PAGE (When Data Entered)

REPORT DOCUMENTATION PAGE

READ INSTRUCTIONS BEFORE COMPLETING FORM

1. REPORT NUMBER: AFML-TR-76-92
2. GOVT ACCESSION NO.
3. RECIPIENT'S CATALOG NUMBER
4. TITLE (and Subtitle): Three-Dimensional Finite Element Stress Analysis of Laminated Plates Containing a Circular Hole
5. TYPE OF REPORT & PERIOD COVERED: Final Report, 15 Jan [redacted] 15 Jul 15, 1975
6. PERFORMING ORG. REPORT NUMBER
7. AUTHOR(s): Dr. Edmund F. Rybicki; Mr. David W. Schmueser
8. CONTRACT OR GRANT NUMBER(s): F33615-74-C-5096
9. PERFORMING ORGANIZATION NAME AND ADDRESS: Battelle, Columbus Laboratories, 505 King Avenue, Columbus, Ohio 43201
10. PROGRAM ELEMENT, PROJECT, TASK AREA & WORK UNIT NUMBERS: 73400394; 03
11. CONTROLLING OFFICE NAME AND ADDRESS: Air Force Materials Laboratory (AFML/MBM), Air Force Wright Aeronautical Laboratories, Air Force Systems Command, Wright-Patterson AFB, Ohio 45433
12. REPORT DATE: Aug [redacted] 76
13. NUMBER OF PAGES: 55
14. MONITORING AGENCY NAME & ADDRESS (if different from Controlling Office): Air Force Materials Laboratory (AFML/MBM), Air Force Wright Aeronautical Laboratories, Wright-Patterson AFB, Ohio 45433
15. SECURITY CLASS. (of this report): Unclassified
15a. DECLASSIFICATION/DOWNGRADING SCHEDULE
16. DISTRIBUTION STATEMENT (of this Report): Approved for public release; distribution unlimited. 55 p.
17. DISTRIBUTION STATEMENT (of the abstract entered in Block 20, if different from Report): Final rept. 15 Jan-15 Jul 75,
18. SUPPLEMENTARY NOTES
19. KEY WORDS (Continue on reverse side if necessary and identify by block number)

Composites	Thermal Stresses
Laminated Plates	Stacking Sequence
Three-Dimensional Stress Analysis	Lay-up Angles
Finite Elements	Stress Concentration
Laminated Plate Theory	Interlaminar Stresses

20. ABSTRACT (Continue on reverse side if necessary and identify by block number)

One of the modes of failure of laminated plates is delamination which initiates at a free edge. Experimental results and theoretical stress analyses found in the literature point to the interlaminar normal stress σ_{zz} as a governing factor for this mode of failure. In this report, the stress behavior around a circular hole in a laminated plate is investigated using a three-dimensional finite element stress analysis. Attention is focused on the interlaminar normal stress distribution around the edge of the circular hole. Graphite

CONT ON NEXT P

DD FORM 1 JAN 73 1473 EDITION OF 1 NOV 65 IS OBSOLETE

UNCLASSIFIED
SECURITY CLASSIFICATION OF THIS PAGE (When Data Entered)

407 080

20. epoxy laminates of the type $(0_2/\pm\theta/\mp\theta)_s$, $(90_2/\pm\theta/\mp\theta)_s$, $(\pm\theta/\mp\theta/0_2)_s$, and $(\pm\theta/\mp\theta/90_2)_s$ where θ is 30°, 45°, and 60°, were modeled. Two types of loadings were considered. One was a uniform stress applied distant to the hole. The other was a uniform temperature change to represent the thermal portion of the laminate fabrication process. Other laminates of the type $(0/90)_s$, $(90/0)_s$, $(0_2/\pm45/\bar{0})_s$, and $(\pm45/0_2/\bar{0})_s$ were considered. In total, results for over thirty laminates are presented. Most of the results are in tabular form.

The influence of stacking sequence, lay-up angle, and ratio of laminate thickness-to-hole diameter on the interlaminar normal stress were examined. The thermal loading condition was selected to provide insight into the residual stress pattern that exists around a circular hole due to curing the laminate. Comparisons of two-dimensional (laminated plate theory) solutions and the three-dimensional finite element results are also compared with experimental results for the tangential strain distribution around a circular hole in a laminated plate. Lastely, an approximate analysis for predicting the sign of the interlaminar normal stress σ_z is presented and comparisons are made with the three-dimensional results.

FOREWORD

This final report was submitted by Battelle's Columbus Laboratories, 505 King Avenue, Columbus, Ohio 43201, under Contract No. F33615-74-C-5096, with the Mechanics and Surface Interactions Branch, Nonmetallic Materials Division, Air Force Materials Laboratory, Wright-Patterson Air Force Base, Ohio. Dr. N. J. Pagano, AFML/MBM, was the Project Monitor.

Dr. Edmund F. Rybicki and Mr. David W. Schmueser were the principal investigators.

TABLE OF CONTENTS

LIST OF ILLUSTRATIONS

LIST OF TABLES

SECTION I

INTRODUCTION

One of the unique characteristics of laminated composite materials is the delamination mode of failure that occurs at free edges. This behavior has been investigated experimentally and by mathematical stress analysis models for laminates with straight free edges. Experimental studies by Pipes, Kaminski, and Pagano[1]* have shown that the laminate stacking sequence can effect the static strength of laminates. Similar effects of stacking sequence were found by Foye and Baker[2] for fatigue loading conditions. Mathematical stress analyses of laminated plates with straight free edges have shown that changes in stacking sequence can alter the behavior of the interlaminar stresses. In particular, investigators[3,4,5] have found that the sign of the transverse normal stress σ_z changes from tension to compression as the stacking sequence is changed. Pagano and Rybicki[6] found that a change in stacking sequence of the type (0°/Matrix), to $(\text{Matrix}/0°)_s$ reversed the sign and changed the magnitude of the interlaminar stress, σ_z. Furthermore, Pagano and Pipes[7,8] have shown that high tensile stresses are associated with the decreased laminate strengths reported in References [1] and [2]. These observations point to the importance of understanding the stress behavior of laminates near a free edge. Through such an understanding, Lackman and Pagano[9] have successfully reduced interlaminar stresses at straight free edges to suppress the delamination mode of failure.

While the straight free edge can be studied as a problem with two-dimensional variations in stresses and displacements, the curved free edge is inherently a three-dimensional problem. Thus, the circular hole problem is more difficult to treat in terms of a mathematical-stress analysis than the straight free-edge problem. Dana and Barker[10] have investigated the three-dimensional stress analysis of four-ply $(0/90)_s$ and $(45/-45)_s$ laminates with circular holes and found that the sign and magnitude of the σ_z distribution around the hole can be changed by altering the stacking sequence. Rybicki and Hopper[11] have developed an analysis for the interlaminar stress distributions

---

* Numbers in brackets denote references given at the end of the report.

for a six-ply symmetric laminate containing a circular hole. Experimental investigations by Daniel, Rowlands, and Whiteside[12] on the effects of stacking sequence on the strength of laminated plates with holes showed that variations in stacking sequence effected the laminate strength and failure mode.

Other studies for example by Greszczuk[13], Waddoups, et al.[14], Waszczuk and Cruse[15], and Whitney and Nuismer[16] have predicted failure of a composite plate containing a hole and made comparisons with experimental data. References [13] and [14] are concerned with predicting failure for damage due to inplane stresses. The stress analyses for these studies did not include interlaminar stresses and thus are not directly applicable to the delamination problem.

There are several basic studies that can provide insight into understanding laminate behavior near a curved-free edge. Five such studies are considered here. The first study concerns the effect of stacking sequence on the transverse stresses. For the problem of the straight free edge, References [3] through [9] point out that changing the stacking sequence can change both the sign and magnitude of the interlaminar stress distribution. However, in the case of a laminate containing a circular hole, the effect of changing the stacking sequence is not understood as well. The second study considers the influence of lay-up angle on the interlaminar stress around circular holes. The third study pertains to the state of residual stresses that exist in the laminate due to the temperature changes in the fabrication process. In the fourth study, the inplane stress distributions around the circular hole obtained from a three-dimensional model are compared with two-dimensional model results obtained from a laminated plate theory model. In the fifth study, the effect of laminate thickness on transverse stresses for a plate with a given hole size is examined for a selected laminate. This problem is of primary importance in the mathematical modeling of laminated plates because a thin plate with a large hole can present high element aspect ratios or a large number of elements in a finite element analysis. In addition, a comparison of predicted and measured strains around a circular hole and an approximate method for predicting the sign of the interlaminar stress, σ_z, are presented. These topics are an important step toward obtaining a better understanding of the behavior of laminates containing a hole and are pertinent to designing laminated structural components as well as to designing test specimens and interpreting laboratory test results.

SECTION II

METHOD OF STRESS ANALYSIS

The method-of-stress analysis is based on a compatible finite element representation for the deformations of a three-dimensional solid. The computer program is SAP IV. Details of this program and the stress analysis method are given in Reference [17]. A summary of the analysis is given here as background information.

In the finite element stress analysis plys are modeled as three-dimensional homogeneous orthotropic materials with linear stress-strain behavior. Symmetric laminates are considered with applied stress loading conditions distant to the hole. The analysis is based on a three-dimensional finite element representation for the displacements within each element. Compatibility conditions within each element and between contiguous elements are satisfied exactly. Equilibrium is satisfied approximately. A twenty-node element with corner and midside nodes was used.

Material properties are based on effective modulus representations for the plys. This representation does not recognize fiber size and geometry. However, effects of such characteristics can be evaluated through the approach described by Rybicki and Pagano[18].

SECTION III

NUMERICAL RESULTS

This section contains numerical results for cases selected to address the question concerning effects of stacking sequence, lay-up angle, thermally induced residual stresses, and laminate thickness on the stress distribution around a hole in a laminated plate. In addition, some comparisons of three-dimensional and two-dimensional laminated plate theory solutions are given.

The numerical results presented in this section are based on seven laminates with different lay-ups. Each laminate was subjected to a mechanical stress loading and three of the laminates were selected for a thermal loading condition. In addition, each of these ten cases were run for a different stacking sequence. Thus, a total of twenty analyses were performed. Because of symmetry, only one quarter of the top half of each laminate was modeled. In each case, a thirty-six element grid with three elements through the thickness and twelve in the laminate plane, as shown in Figure 1, was used to model one eighth of the laminate.

1. Effect of Stacking Sequence

The effect of stacking sequence has been an important topic of study for free-edge problems. As stated previously, the effects of stacking sequence on a circular free edge are not as well understood as for the case of the straight free edge. To provide more insight into this problem, seven laminates with a mechanical stress loading condition and three laminates with a thermal stress loading condition were considered. Results were also obtained for the associated ten cases with different stacking sequences.

The lay-up for the first laminate was $(0/90)_s$. Ply properties for the 0° ply are given in Table 1. The applied stress boundary conditions were selected to produce a unit average stress parallel to the 0° direction or in the y direction illustrated in Figure 1. The applied stresses are given in Table 2. The convention for lay-up angles is that angles are measured clockwise from the load direction. A laminate thickness to hole diameter ratio of

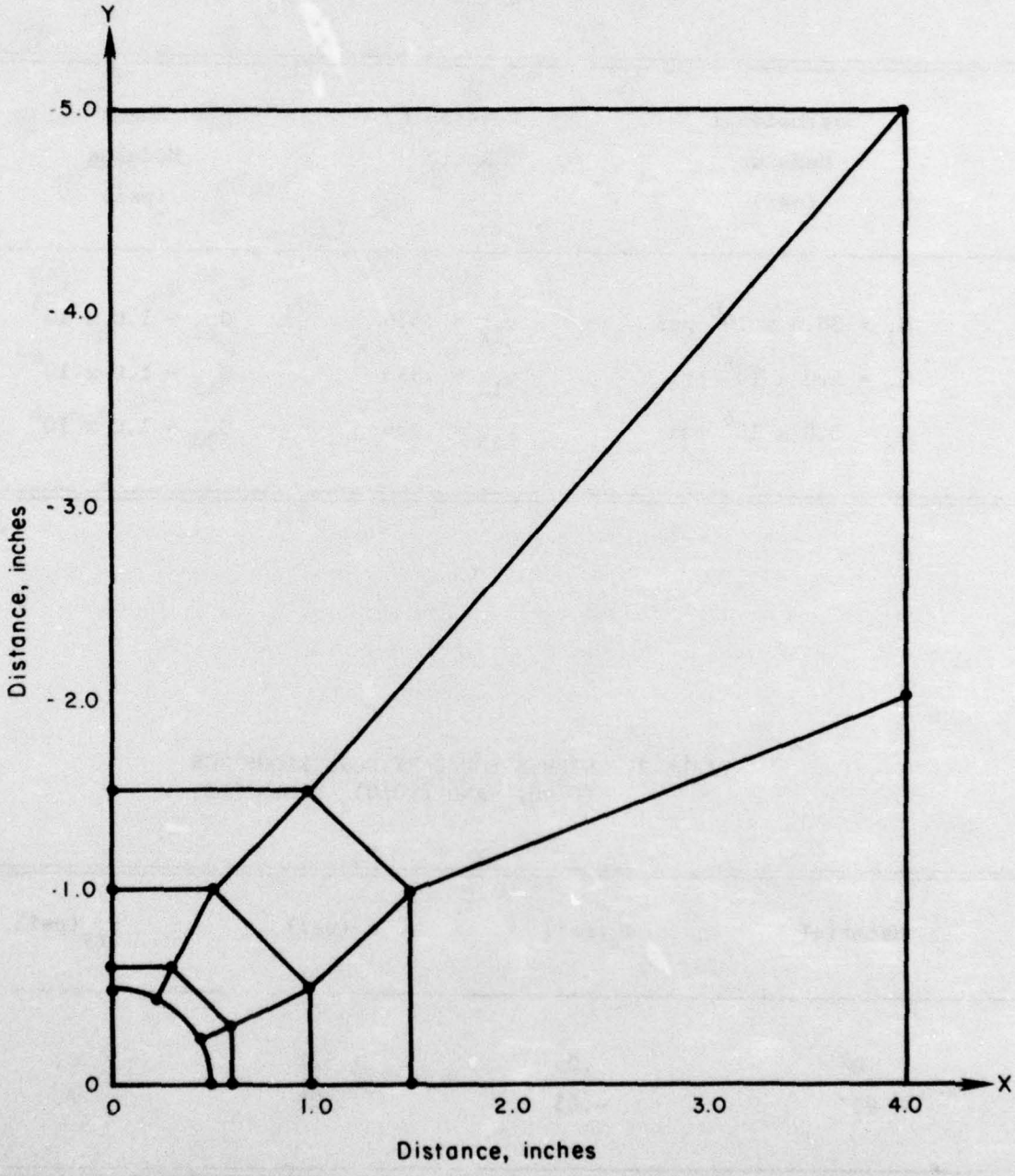

FIGURE 1. FINITE ELEMENT GRID IN THE X-Y PLANE

TABLE 1. MATERIAL PROPERTIES OF THE 0° LAMINA IN THE $(0/90)_s$ LAMINATE.

Extensional Modulus (psi)	Poisson's Ratio	Shear Modulus (psi)
$E_1 = 30.0 \times 10^6$ psi	$\nu_{12} = .336$	$G_{12} = 1.0 \times 10^6$
$E_2 = 3.0 \times 10^6$ psi	$\nu_{13} = .336$	$G_{13} = 1.0 \times 10^6$
$E_3 = 3.0 \times 10^6$ psi	$\nu_{23} = .336$	$G_{23} = 1.0 \times 10^6$

TABLE 2. STRESS BOUNDARY CONDITIONS FOR $(0/90)_s$ AND $(90/0)_s$ LAMINATES.

Material	σ_x(psi)	σ_y(psi)	τ_{xy}(psi)
0°	.05	1.821	0.
90°	-.05	.179	0.

.8 was selected. The results for the σ_z distribution around the circular hole at the laminate midplane are shown in Figure 2. Two important results are shown in this figure. First, the stress distribution changes sign and magnitude as the stacking sequence is changed. Second, the sign of σ_z at $\theta = 90$ for these $(90/0)_s$ and $(0/90)_s$ laminates can be predicted from the sign of the moment away from the circular hole along $\theta = 90$, by using equilibrium considerations on the remote applied stresses, but this is not true at $\theta = 0°$ where the sign of the moment due to remote stresses would always indicate a tensile stress for σ_z.

Six other laminates were considered. These were of the type $(\pm\theta/\mp\theta/0_2)_s$ and $(\pm\theta/\mp\theta/90_2)_s$ where θ is 30°, 45°, and 60°. Stacking sequences were changed by reversing the $(\pm\theta/\mp\theta)$ plys and the (0_2) or (90_2) plys. The (0_2) and (90_2) plys were modeled as one material and the $(\pm\theta/\mp\theta)$ plys were modeled as a single material with effective modulus properties. Table A-1 of Appendix A contains the properties obtained from Reference [19] and used in this part of the study. A unit stress in the 0° direction was applied to each laminate. The stress boundary conditions for each laminate are given in Table A-2 of Appendix A. In addition to the unit stress loading, the effect of stacking sequence for a thermal loading of -200 F was also considered. Coefficients of linear thermal expansion shown in Table A-1 were used in this calculation. For the thermal loadings, only the last three laminates designated in Table A-2 were considered because in terms of the models, the last three laminates are equivalent to the first three rotated by 90°. For both mechanical and thermal loading conditions, a hole diameter of 1 inch and laminate thickness of .6 inch was used.

Tables A-3 through A-8 of Appendix A contain stresses at the laminate midplanes for a unit stress applied parallel to the 0° direction. Reference will be made to these tables to describe some of the characteristics of the stress distribution for the interlaminar stress denoted by σ_z. Comparison of Tables A-3 and A-6 and Tables A-4 and A-7 show that for the $(\pm\theta/\mp\theta/0_2)_s$ to $(0_2/\mp\theta/\pm\theta)_s$ changes in stacking sequence, the sign and magnitude of the σ_z stress distribution at the laminate midplane is changed. It is noted that the σ_z stresses for the $(0_2/\pm\theta/\mp\theta)_s$ laminates are generally lower than the values for the $(\pm\theta/\mp\theta/0_2)_s$ laminates.

The $(\pm 30/\mp 30/90_2)_s$ and $(\pm 45/\mp 45/90_2)_s$ laminates display a σ_z distribution that is totally tension around the edge of the hole as seen from the results in Tables A-4 and A-5. The effect of changing stacking sequence is to change

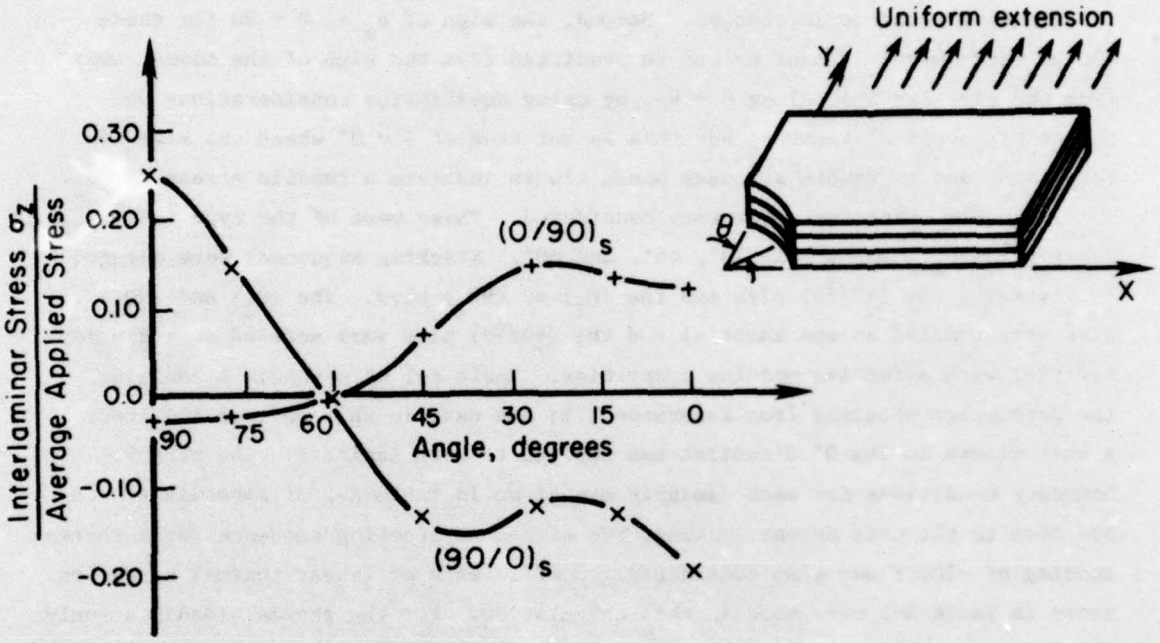

FIGURE 2. INTERLAMINAR STRESS σ_z FOR UNIFORM EXTENSION OF $(0/90)_s$ and $(90/0)_s$

this distribution to totally compression as seen in Tables A-7 and A-8. The σ_z distribution for the $(\pm 60/\mp 60/90_2)_s$ laminate (Table A-5) has a sign change from compression to tension in going from 0° to 90°. The associated $(90_2/\pm 60/\mp 60)_s$ laminate (Table A-8), however, does not show this sign change. The results show larger values for σ_z in the $(\pm\theta/\mp\theta/90_2)_s$ laminates than in the $(90_2/\pm\theta/\mp\theta)_s$ laminates.

The effects of changes in stacking sequence for thermal loading is shown by the results in Tables A-9, A-10, and A-11. Once again, a change in both sign and magnitude are found for changing stacking sequence. Several interesting features of these results are noteworthy. The $(\pm 30/\mp 30/90_2)$ and the $(90_2/\pm 30/\mp 30)_s$ laminates show a change in sign of σ_z in going from $\theta = 0°$ to 90°. The $(\pm 45/\mp 45/90_2)_s$, $(90_2/\pm 45/\mp 45)_s$, $(\pm 60/\mp 60/90_2)_s$, and $(90_2/\pm 60/\mp 60)_s$ laminates do not show this sign change. Generally, higher values of σ_z occur for the (90_2) ply in the center. The two laminates with $(\pm 60/\mp 60)$ show relatively flat distribution for σ_z as a function of angle. The $(90_2/\pm 45/\mp 45)_s$ shows the highest value of tensile σ_z. Finally, it is noted that the peak values of σ_z do not always occur at $\theta = 0°$ or at $\theta = 90°$.

2. Effect of Lay-Up Angle

Results showing the effect of lay-up angle for $(0_2/\pm\theta/\mp\theta)_s$, $(90_2/\pm\theta/\mp\theta)_s$, $(\pm\theta/\mp\theta/0_2)_s$, and $(\pm\theta/\mp\theta/90_2)_s$ laminates are shown in Tables A-3 through A-11. One obvious effect of increasing the lay-up angle is the increase in the peak tangential stress (at $\theta = 90°$) in the center plys for the case where the (90_2) or (0_2) plys are in the center of the laminate. Peak compressive and tensile values of σ_z for the $(\pm\theta/\mp\theta/0_2)_s$ laminates are relatively close together. Peak values of tensile stress are highest for the $(\pm 45/\mp 45/90_2)_s$ and $(\pm 60/\mp 60/90_2)_s$ laminates. For the laminates with the (0_2) plys on the outside, the peak values of σ_z generally increase for increasing values of θ. For the thermal loadings considered, the effect of changing lay-up angle is to change the character of the σ_z distribution around the hole. This is seen in Tables A-9 through A-11 for the $(\pm\theta/\mp\theta/90_2)_s$ laminates. Of the three $(90_2/\pm\theta/\mp\theta)_s$ laminates considered, the maximum value of tensile σ_z occurs for the case $\theta = 45°$. The effects of lay-up angle also change σ_θ in magnitude and sign as seen for the thermal loading conditions shown in Tables A-9 through A-11.

3. Residual Stresses Due to Fabrication

Graphite/epoxy laminates are cured at an elevated temperature. Cooling to room temperature can cause residual stresses in the laminate due to the mismatch in the coefficients of thermal expansion. To obtain an estimate of the magnitude and distribution of these stresses, three laminates were modeled for a temperature loading condition of -200 F. The material properties are shown in Table A-1. The boundary conditions were stress free. Tables A-9 through A-11 show the stress results at the laminate midplane for $(\pm\theta/\mp\theta/90_2)_s$ and $(90_2/\pm\theta/\mp\theta)_s$ laminates. The highest tensile value for σ_θ is 9570 psi and occurs in the (90_2) plys of the $(\pm 60/\mp 60/90_2)_s$ laminate. The highest compressive sive value of σ_θ is 11,560 psi and occurs in the (90_2) plys of the $(\pm 30/\mp 30/90_2)_s$ laminate. Tensile values of σ_z from 800 psi to 1815 psi are predicted for the six cases with the maximum value occurring for the $(\pm 30/\mp 30/90_2)_s$ laminate. The magnitudes of the predicted transverse stresses are approaching values large enough so that they cannot be neglected compared to the transverse strength of the laminate.

4. Comparison of LPT and Three-Dimensional Stress Distributions

One stress analysis approach that is commonly used for fiber reinforced plates is based on the laminated plate theory (LPT). A description of the method can be found in many references, for example, see Reference [18]. In the LPT models, the out-of-plane stresses are zero. LPT analyses are used in the design of composite structures to predict their survivability. Thus, it is of interest to know how the LPT stresses compare with the three-dimensional stress distributions. In the far-field regions, away from edges and attachments, the LPT solution is exact for linear elastic behaivor. Near free edges, the boundary conditions of the LPT solution are that the resultant force and bending moments on the edges are zero. The LPT model permits nonzero stresses on the laminate free edges while the true boundary conditions are zero normal and shear stresses on these edges.

In this study, the tangential stress distributions around a circular hole for several laminates was obtained by the LPT model and compared with the tangental stress distributions from the three-dimensional finite element solutions obtained by the SAP IV program. The LPT solutions were obtained by

evaluating the effective modulii of the laminate and using these properties in a two-dimensional solution for an orthotropic plate containing a hole. These properties are given in Table A-1 of Appendix A. The stress distributions obtained from the orthotropic plate analysis are resultant stresses. The stresses in each ply can then be evaluated from the LPT distributions by using the conditions that the inplane strains are the same in all plys. Comparisons of the tangential stress distributions around circular holes were made with results obtained from the three-dimensional finite element stress analysis and results from the LPT model. Twelve laminates and the three-dimensional results are given in Tables A-1 thrugh A-8. A summary of these results and the LPT results are shown in Tables A-12 through A-14. Note that the LPT solution is independent of stacking sequence and stresses do not vary through the thickness of the ply. This is not the case for the three-dimensional finite element results. Thus, a plane had to be selected in the three-dimensional model for comparison with the LPT results. The midplane of the laminate was selected as the location for obtaining the three-dimensional results. The reason for this was that the tangential stresses at this location appeared to take on the largest magnitudes. A summary of comparisons for σ_θ given in Tables A-12, A-13, and A-14. Note that the stresses for the $(\bar{\mp}\theta)$ ply were evaluated from $(0_2/\underline{\pm}\theta/\bar{\mp}\theta)_s$ or $(90_2/\underline{\pm}\theta/\bar{\mp}\theta)_s$ laminates while the stresses for the (0_2) and (90_2) plys were evaluated from $(\underline{\pm}\theta/\underline{\pm}\theta/0_2)_s$ and $(\underline{\pm}\theta/\bar{\mp}\theta/90_2)_s$ laminates. The greatest variation between these two results occurs in the (0_2) plys of the $(\underline{\pm}\theta/\bar{\mp}\theta/0_2)_s$ laminates. The differences between the results for the (90_2) and $(\bar{\mp}\theta)$ plys in the $(\underline{\pm}\theta/\bar{\mp}\theta/90_2)_s$ laminates is about the same magnitude.

Two additional laminates were considered in this study to further illustrate the comparison of three-dimensional finite element results and LPT solutions. The lay-up is denoted by $(0_2/\underline{\pm}45/\bar{0})_s$ and $(\underline{\pm}45/0_2/\bar{0})_s$. For this laminate, the properties used for the $(\underline{\pm}45)$ plys and the 0° plys are given in Table 3. Note that the $(\underline{\pm}45)$ plys were represented by as a single material with no extensional/bending coupling. Also, the value for ν_{12} of .778 is less than what would be obtained by rotating the properties for the 0° ply given in Table 3. Nonetheless, these properties have some value in comparing two- and three-dimensional solutions. Figure 3 shows a comparison of the tangential stress distributions obtained from the three-dimensional and two-dimensional analyses for the $(0_2/\underline{\pm}45/\bar{0})_s$ laminate. These differences are of the same order

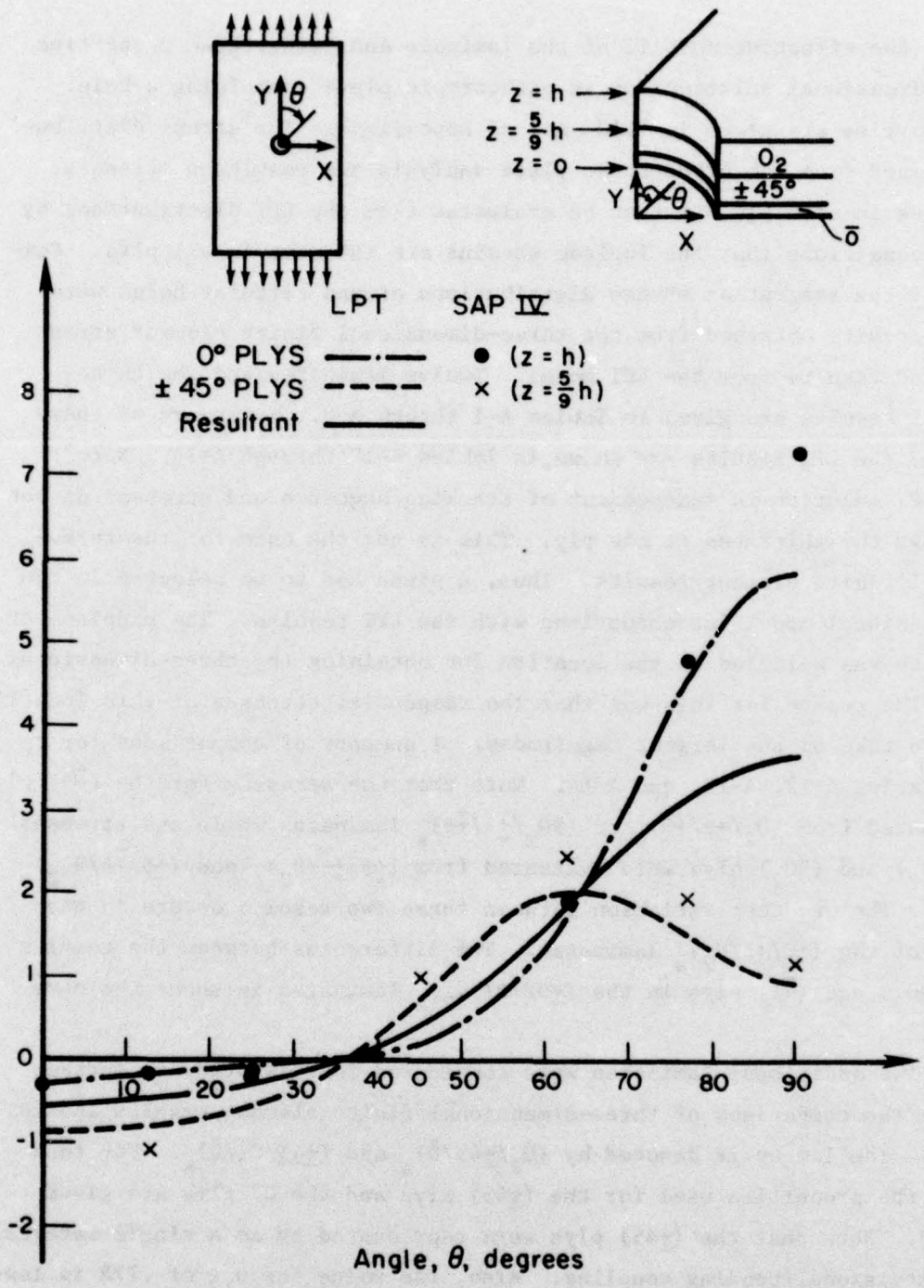

FIGURE 3. STRESS DISTRIBUTIONS AROUND A HOLE IN A $(0_2/\pm 45/\bar{0})_s$ LAMINATE

TABLE 3. MATERIAL PROPERTIES USED IN MODELING $(0_2/\pm45/\bar{0})_s$ AND $(\pm45/0_2/\bar{0})_s$ LAMINATES

	Modulus (10^6 psi)	Poisson's Ratios	Shear Modulus (10^6 psi)
0° Plys	$E_1 = 30.0$	$\nu_{12} = .21$	$G_{12} = 1.06$
	$E_2 = 2.7$	$\nu_{13} = .24$	$G_{13} = 1.06$
	$E_3 = 2.7$	$\nu_{23} = .25$	$G_{23} = 1.06$
(±45) Plys	$E_1 = 3.77$	$\nu_{12} = .778$	$G_{12} = 7.92$
	$E_2 = 3.77$	$\nu_{13} = .21$	$G_{13} = 1.06$
	$E_3 = 2.7$	$\nu_{23} = .21$	$G_{23} = 1.06$

as those shown in Tables A-12, A-13, and A-14. Figure 4 is of more interest in that it shows how the tangential stress distribution through the laminate thickness and compares this with the LPT solution. The most pronounced difference appears to be that the stress "concentration" for the 0° plys is higher in the three-dimensional analysis than in the two-dimensional analysis.

5. Effects of Laminate Thickness to Hole Radius Ratio

In the case of a straight-free edge, the only factor changing the inplane stresses is the free edge. For the case of the circular hole, the in plane stresses are alao influenced by the stress concentration due to the hole. In the two-dimensional solution for plate containing a circular hole, the region of influence depends on the hole radius and the material properties. Also, the gradient of the inplane stress, σ_θ, is very steep along the direction perpendicular to the direction of loading. Thus, several distinct characteristics of the circular free-edge problem do not appear in the straight free-edge problem. For this reason, it is not obvious that the circular free edge behaves like the straight free edge even for small laminate thickness to hole radius ratios. Thus, the ratio of laminate thickness to hole radius becomes an important parameter to study in obtaining a basic understanding of the

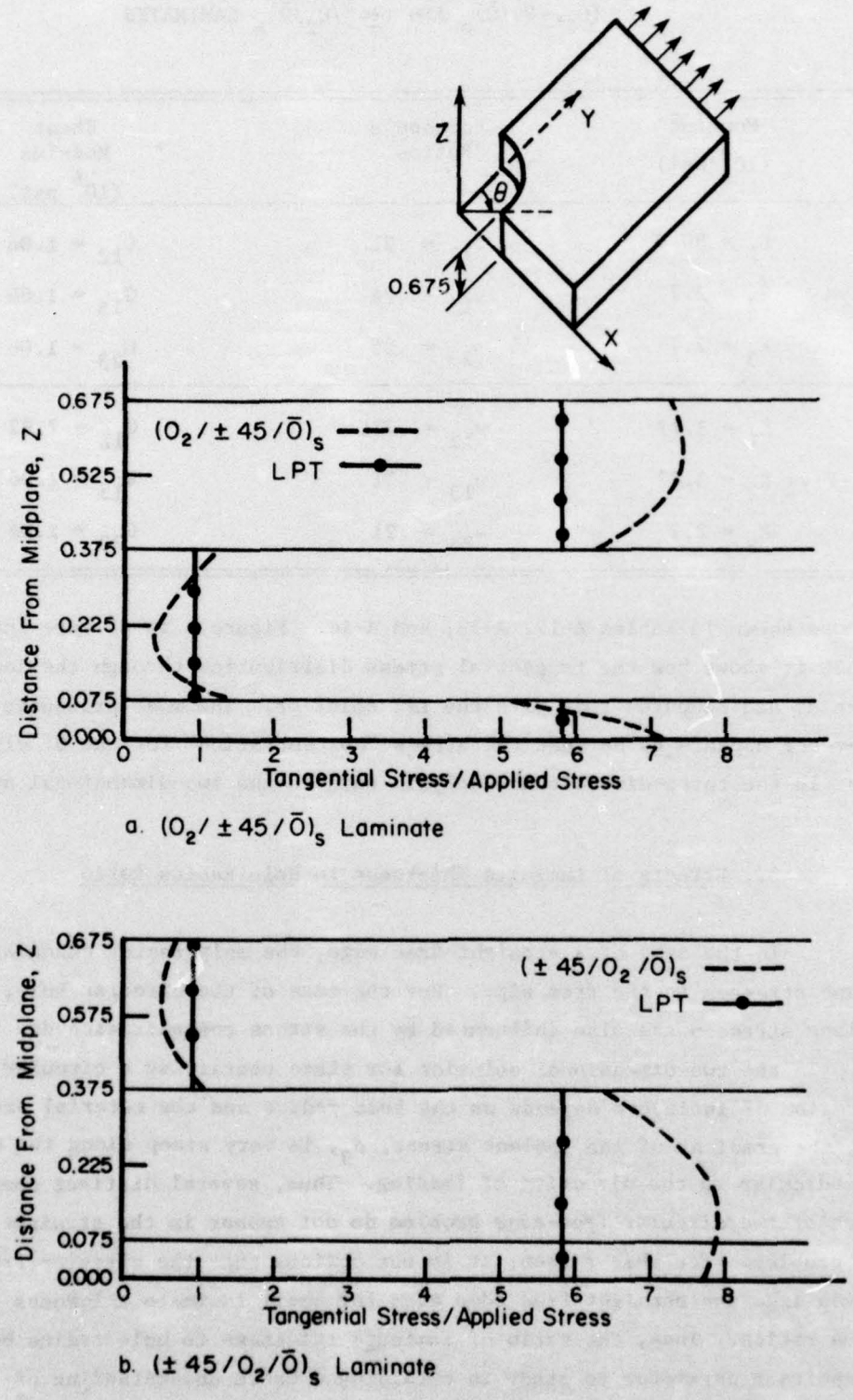

FIGURE 4. DISTRIBUTION OF TANGENTIAL STRESS THROUGH LAMINATE THICKNESS AT θ = 90°

behavior around a circular hole. An other reason for examining the influence of this parameter is related to the feasibility of obtaining numerical solutions. The finite elements must not exceed a certain aspect ratio to maintain numerical stability of the solution technique. Thus, modeling individual boron or graphite laminas, which are .005 to .008 inch thick, could require more finite elements than is feasible. However, for thick laminates where the lamina thickness to hole radius ratio is .5, the aspect ratio requirements can be met with a feasible number of elements. Thus, if the solution for a thick laminate is easier to obtain or the only solution available, it is important to understand how the thick plate is related to the solutions for a thinner laminate.

To help understand this relationship, a laminate containing a 1-inch hole was considered. This laminate consists of two materials denoted by PLYA and PLYB. The lay up for this laminate is $(PLYB_2/PLYA_5/PLYB_2)$. Properties for these two materials are given in Table 4. The hole size was kept constant and the thickness of the laminate was allowed to vary from 1.8 inches to .45 inch.

TABLE 4. MATERIAL PROPERTIES FOR THE STUDY OF EFFECTS OF LAMINATE THICKNESS-TO-HOLE RADIUS RATIO $(PLYB_2/PLYA_5/PLYB_2)$

Ply Designation	Extensional Modulus (psi)	Poisson's Ratio	Shear Modulus (psi)
PLYA	$E_1 = 30.0 \times 10^6$	$\nu_{12} = .25$	$G_{12} = .65 \times 10^6$
	$E_2 = 2.7 \times 10^6$	$\nu_{13} = .25$	$G_{13} = .65 \times 10^6$
	$E_3 = 2.7 \times 10^6$	$\nu_{23} = .25$	$G_{23} = .5 \times 10^6$
PLYB	$E_1 = 2.08 \times 10^6$	$\nu_{12} = .598$	$G_{12} = 2.38 \times 10^6$
	$E_2 = 2.08 \times 10^6$	$\nu_{13} = .136$	$G_{13} = 5.65 \times 10^6$
	$E_3 = 2.7 \times 10^6$	$\nu_{23} = .136$	$G_{23} = 5.65 \times 10^6$

Because of symmetry, only one-eighth of the laminate was considered in the finite element representation. This is one quarter of the top half of the laminate. Thirty-six elements were used in this model. Three elements through the thickness and twelve elements, as shown in Figure 1, were used in the plane of the laminate. The loading conditions were presecribed stresses on the boundaries to represent the laminated plate theory solution for a uniform average stress of unity in the 1 direction. The applied stresses are given in Table 5.

TABLE 5. STRESS BOUNDARY CONDITIONS FOR THE $(PLYB_2/PLYA_5/PLYB_2)$ LAMINATE

Material	σ_2 (psi)	σ_1 (psi)	τ_{12} (psi)
PLYB	.033	.137	0.
PLYA	-.026	1.690	0.

Four cases were run with thickness to diameter ratios of 1.80, 1.35, .9, and .45. The tangential stress distribution around the circular hole at the laminate midplane is shown in Figure 5 for a ratio of 0.9. The tangential stress distribution for the other three cases did not vary by more than .98 which is 10 percent of the maximum value at θ = 90 shown in Figure 5. The values for the maximum σ_θ decreased with decreasing T/D to a value of 8.8 for T/D = equal to .45. The tangential stress distribution at the midplane was selected because the largest values of σ_θ occurred there. The results for σ_z were more sensitive to the changes in thickness. Figure 6 shows the distribution of σ_z around the circular hole at the laminate midplane for the four ratios of thickness to hole diameter, T/D. While the changes in σ_z were small compared to the maximum value of the tangential stress, the changes were larger compared to the magnitude of σ_z. As can be seen from Figure 6, the tensile value of σ_z decreased by 30 percent as the ratio of T/D changed from 1.80 to .45. For this cae, the value of σ_z ranges from -28 to +16 percent of the average applied stress.

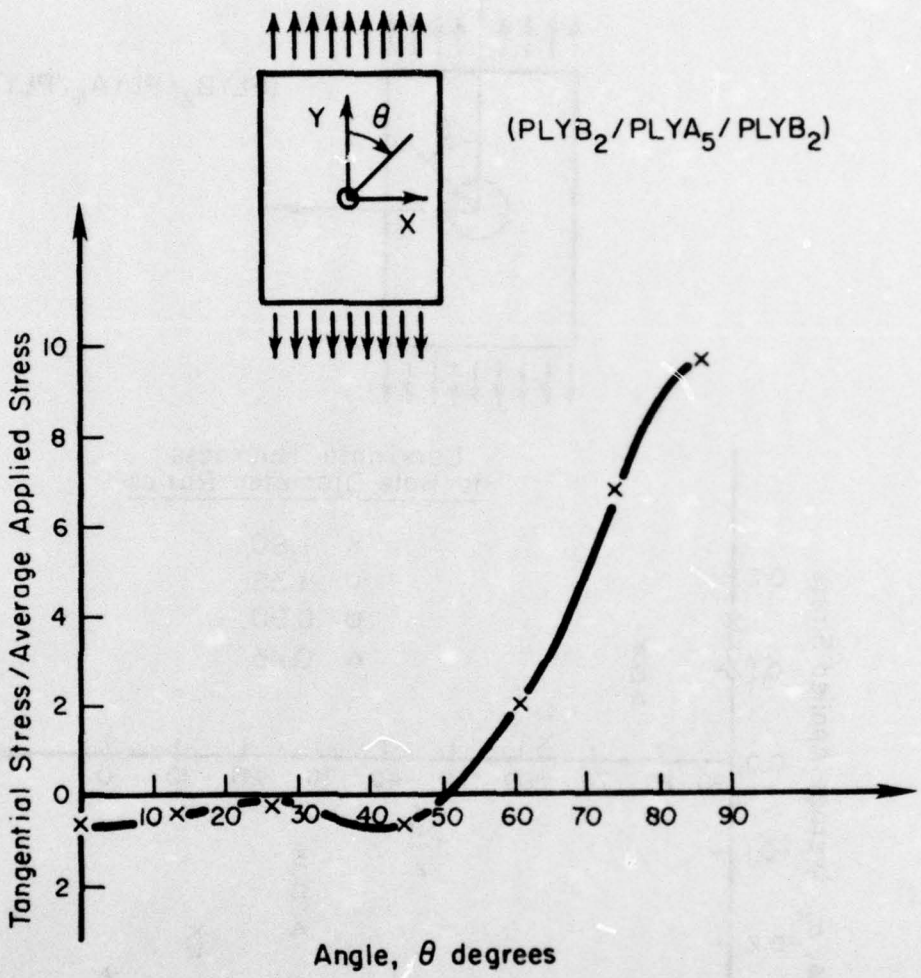

FIGURE 5. STRESS DISTRIBUTION AROUND A CIRCULAR HOLE AT LAMINATE MIDPLANE FOR 0° CENTER PLY

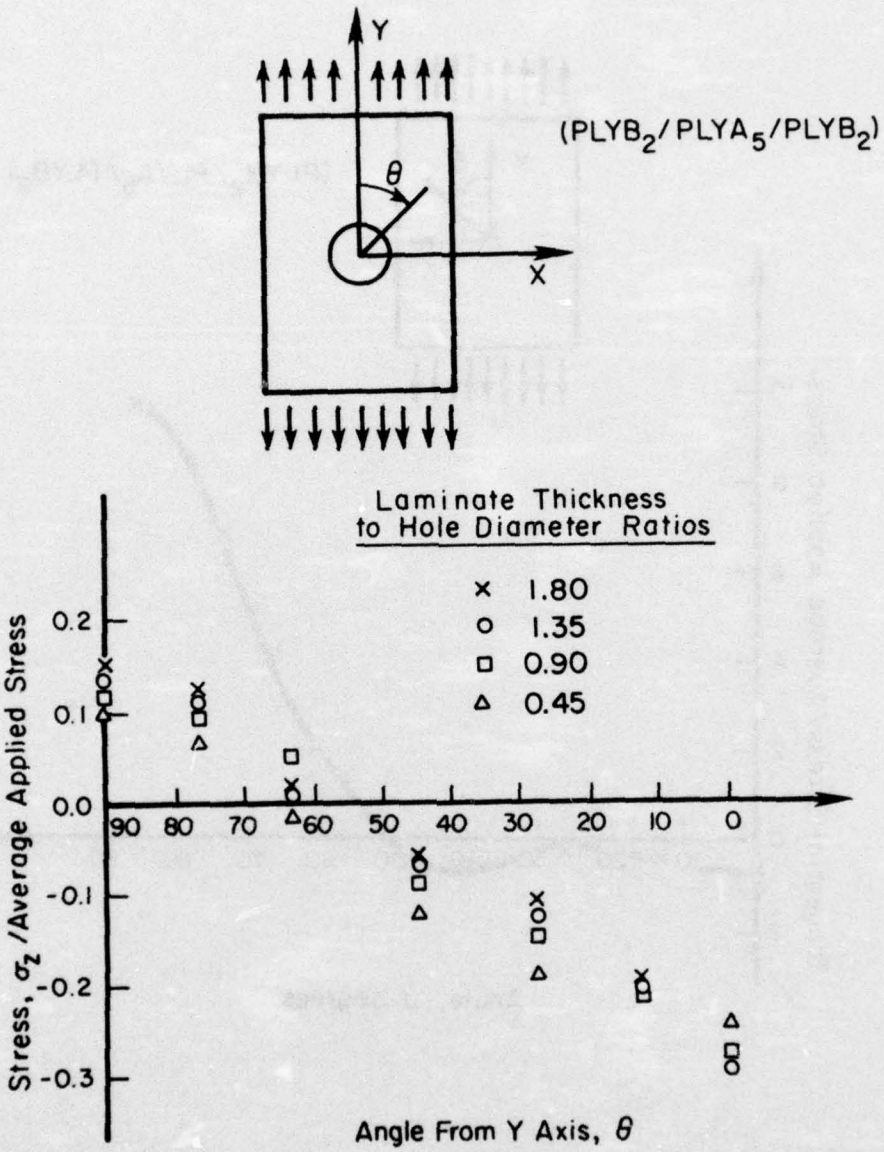

FIGURE 6. DISTRIBUTION OF INTERLAMINAR STRESS σ_z AT LAMINATE MIDPLANE AROUND A CIRCULAR HOLE

SECTION IV

COMPARISON WITH EXPERIMENTAL RESULTS

In this section, a comparison of experimental data and results from the three-dimensional finite element model and the LPT model are presented for a $(0_2/\pm 45/\bar{0})_s$ laminate. The tangential strain distribution around the circular hole was selected for the comparison. Data were obtained from References [12] and [21]. The properties in the material direction used in the analysis are given in Table 3. In the three-dimensional finite element model, the ($\pm$ 45°) plys were treated as a single material. The tangential strain distribution, ε_θ, was obtained and divided by the far-field strain in the direction of the loading. The experimental results were obtained using the measured strain concentration factors in Reference [12] at 0° and 90°. Data for intermediate angles were based on the birefringence data distributions in Reference [12] for the lowest loading level. In addition, the tangential strain distribution based on the LPT model was obtained. The comparison of predicted and measured strain distributions is shown in Figure 7. This figure shows good agreement between all four strain distributions. It also shows that the tangential strain distribution in the ($\pm$45°) plys is not the same as that in the 0° plys. However, the average is close to the values obtained from LPT.

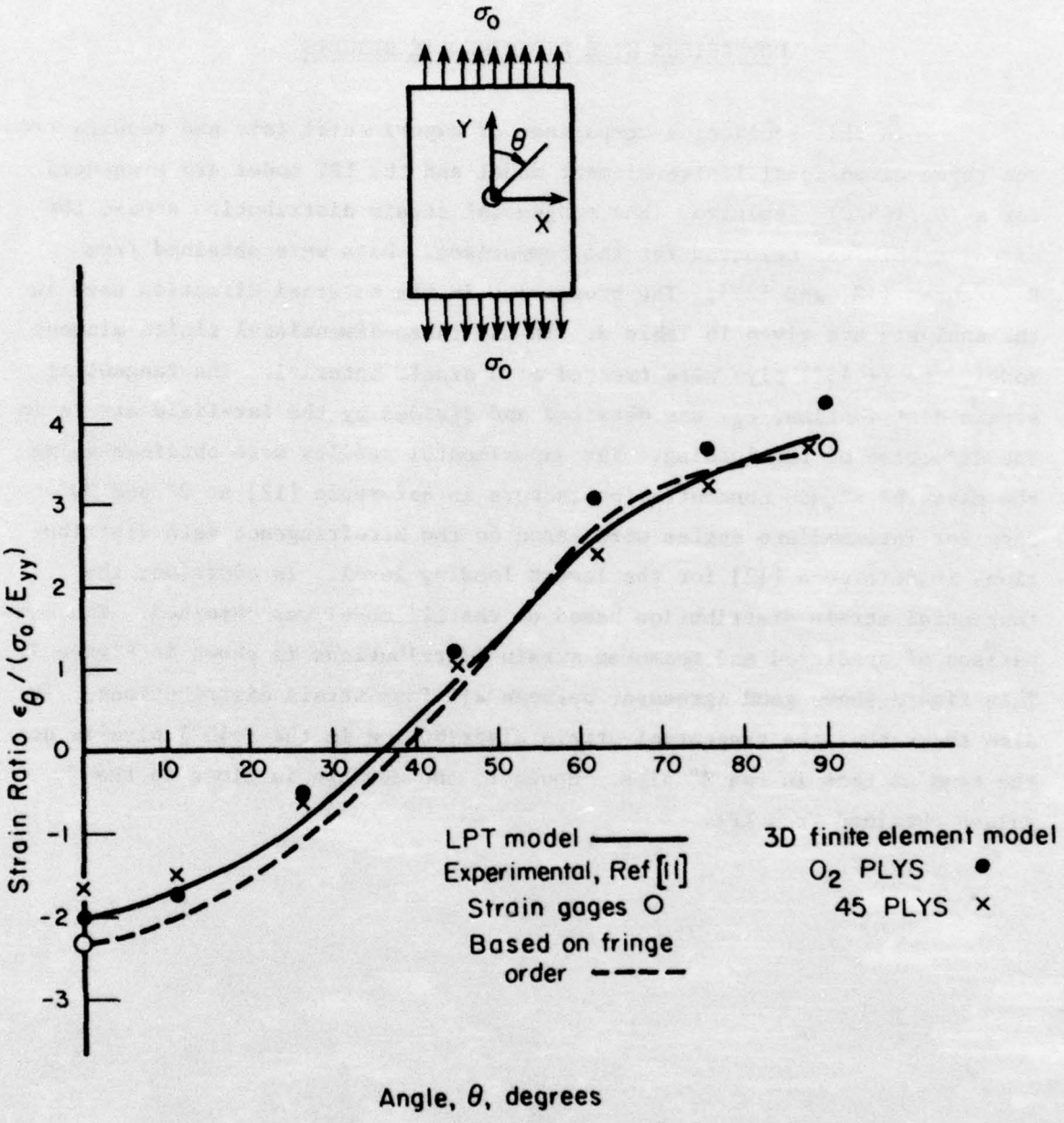

FIGURE 7. TANGENTIAL STRAIN DISTRIBUTIONS AROUND A CIRCULAR HOLE OBTAINED FROM THREE-DIMENSIONAL FINITE ELEMENT MODEL, LPT MODEL AND EXPERIMENTAL DATA FOR A $(0_2/\pm 45/\bar{0})_s$ LAMINATE

SECTION V

APPROXIMATE ANALYSIS FOR THE SIGN OF THE INTERLAMINAR NORMAL STRESS AT MIDPLANE

While the three-dimensional solutions provide a better understanding of the interlaminar stress distribution around holes, one of the reasons for conducting this study is to obtain solutions which can serve as a basis for developing and evaluating simpler stress analysis models. In this section, one such model is presented. This model is very preliminary in the sinse that it is applied to a limited number of problems and based on certain assumptions about the stress behavior of the laminate. Nonetheless, this simple model serves as a starting point for attacking a complex problem. The limitations and assumptions of the models are described in the following. The model is then applied to the stress loaded laminate problems to predict the sign of σ_z at selected points around the free edge. Good quantitative agreement was obtained between the three-dimensional finite element results and the results of the model.

The model is based on an equilibrium description of a wedge shaped section of plate shown in Figure 8. Loading conditions are stresses applied to the boundaries of the plate. Unlike the model of Pagano and Pipes [7], this model is not based on the far field stresses in the loaded plate. The conceptual basis for this model is that the interlaminar stresses around a circular hole can be viewed as a reaction to a set of stresses equal to but having the opposite sign of the edge stresses from the Laminated Plate Theory solution. This concept is implemented in the following three steps. The first step is to obtain a Laminated Plate Theory (LPT) solution for the problem of laminated plate containing a circular hole with stress boundary conditions. The LPT solution gives nonzero stresses, $\sigma_r(\theta)$ and $\tau_{r\theta}(\theta)$, for each ply around the hole. The second step is to impose the negative of these edge stresses on an otherwise stress-free body and determine their effect on the interlaminar stresses through equilibrium considerations. The third and final step is to superimpose these two solutions to obtain an approximate solution for the three-dimensional problem LPT stresses around the circular hole.

Several assumptions concerning the equilibrium of the section shown in Figure 8 are worthwhile to pointing out before writing the equilibrium equa-

tions. First, only two equations are considered. These are statements that the sum of the forces in the z direction are zero and the sum of the moments in the θ direction are zero. The shear stress, $\tau_{\theta z}$, is not included and equilibrium of moments in the r direction is not considered in this simple model. The assumed form for $\sigma_z(r)$ is shown in Figure 8. Due to the simplicity of this model, the results are treated in a qualitative way here and only the sign of σ_z at the radius of the hole is considered. Since σ_z is the only stress contributing to force equilibrium in the z direction, the sign of σ_z at the edge of the hole can be found from the sign of the term in the moment equilibrium equation that is due to $\sigma_z(r)$. As a result of the preceding assumptions, equilibrium equations for the force in the z direction and the moment in the θ direction are given by

$$\int_{\theta=\theta_1}^{\theta_1+\Delta\theta} \int_{r=a}^{R} \sigma_z(r)\, r\,dr\,d\theta = 0 \qquad (1)$$

and

$$\int_{\theta=\theta_1}^{\theta_1+\Delta\theta} \int_{r=a}^{R} \sigma_z(r)\,(r-a)\,r\,dr\,d\theta - \sigma_r(a)\,\frac{h_2}{2}\left\{h_1+h_2\right\} a\Delta\theta$$

$$+ \int_{\theta=\theta_1}^{\theta_1+\Delta\theta} \int_{r=a}^{R} \frac{\partial \tau_{r\theta}}{\partial \theta}\, h_2\, \frac{1}{2}\left\{h_1+h_2\right\} dr\,d\theta = 0 \quad , \qquad (2)$$

where R is selected as the distance from the edge of the hole where the free-edge effects are negligible. The quantities h_1, h_2, and a are shown in Figure 8.

The procedure is to evaluate the second and third terms of Equation (2) using LPT. The sign of σ_z at the edge of the hole was obtained from the sign of the first term in Equation (2). That is, if the first term in Equation (2) is positive, then the σ_z is negative or compressive at the edge of the hole.

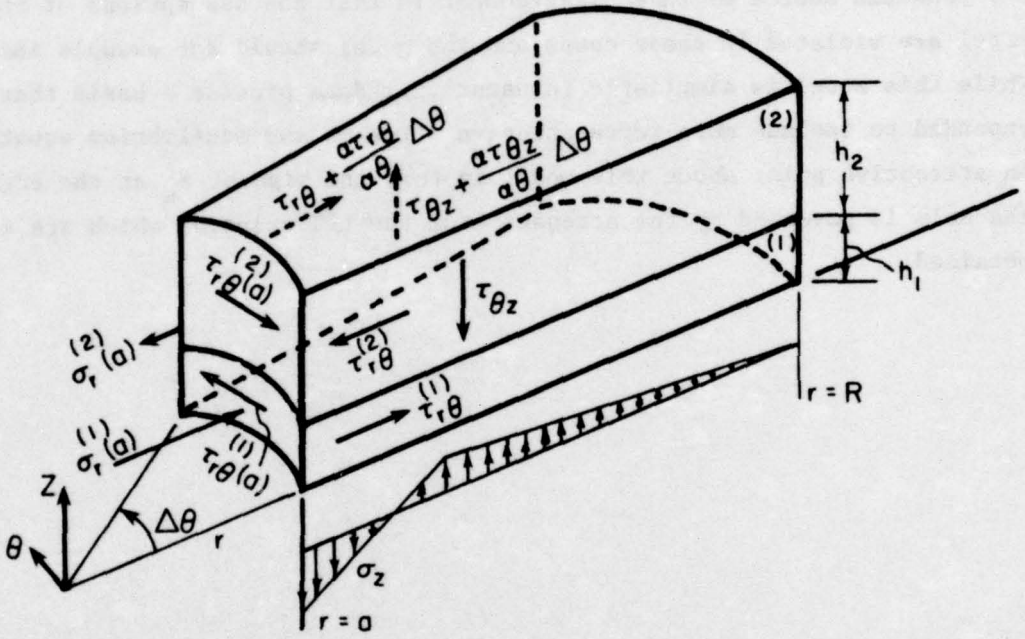

FIGURE 8. FREE BODY DIAGRAM OF MODEL FOR APPROXIMATE ANALYSIS OF INTERLAMINAR STRESSES

Several examples are considered using this model. Results are compared with the three-dimensional finite element solutions and are shown in Table 6. Results for two locations on each laminate are shown in this table. These locations are at the edge of the hole at $\theta = 0$, and $\theta = 90°$. Note that there is agreement between this model and three-dimensional finite element results for $\theta = 90°$. However, at $\theta = 0°$, there is some disagreement for the laminates containing (90_2) plys. There could be several reasons for this. One possible source of this disagreement is that the assumptions of the simple model are violated in these cases and the model should for example include $\tau_{\theta z}$. While this model is simplistic in nature, it does provide a basis that can be expanded to include more representative stresses and equilibrium equations. An attractive point about this model is that the sign of a_z at the edge of the hole is governed by the stresses from the LPT solution which are easily obtained.

TABLE 6. COMPARISON OF SIGNS FOR THE INTERLAMINAR STRESS σ_z OBTAINED FROM THE THREE-DIMENSIONAL ANALYSIS AND AN APPROXIMATE ANALYSIS. T = Tension, C = Compression

Laminate	θ = 0°		θ = 90°	
	Approximate Analysis	Three-Dimensional Analysis	Approximate Analysis	Three-Dimensional Analysis
$(\pm 30/\mp 30/0_2)_s$	C	-.203	T	.149
$(\pm 45/\mp 45/0_2)_s$	C	-.345	T	.186
$(\pm 60/\mp 60/0_2)_s$	C	-.376	T	.161
$(0_2/\pm 30/\mp 30)_s$	T	.068	C	-.081
$(0_2/\pm 45/\mp 45)_s$	T	.181	C	-.062
$(0_2/\pm 60/\mp 60)_s$	T	.233	C	-.086
$(\pm 30/\mp 30/90_2)_s$	C	.051*	T	.255
$(\pm 45/\mp 45/90_2)_s$	C	.025*	T	.659
$(\pm 60/\mp 60/90_2)_s$	C	-.142	T	.716
$(90_2/\pm 30/\mp 30)_s$	T	-.114*	C	-.190
$(90_2/\pm 45/\mp 45)_s$	T	-.135*	C	-.332
$(90_2/\pm 60/\mp 60)_s$	T	-.066*	C	-.262

* Denotes disagreement between sign of σ_z from Approximate Analysis and Three-Dimensional Analysis.

SECTION VI

SUMMARY AND CONCLUSIONS

Three-dimensional finite element solutions for the stress distributions around a circular hole in a laminated plate were presented. Problems were selected to address questions concerning the effects of stacking sequence, lay-up angle, and a uniform temperature change on the inplane and interlaminar stress distributions. A comparison of stresses obtained by the LPT model and the three-dimensional finite element model was made. The effects of the ratio of laminate thickness to hole diameter on the interlaminar stress σ_z was examined. Predicted and measured strain distributions around a circular hole was compared and a preliminary investigation of an approximate model to predict the sign of σ_z was described.

The stress analyses of the laminates were obtained using the SAP IV three-dimensional finite element stress analysis computer program. Conclusions are thusly based upon the laminates selected and the results of the SAP IV finite element program.

The effect of stacking sequence on the interlaminar stress distribution around a circular hole was investigated using $(0/90)_s$, $(90/0)_s$, $(0_2/\pm\theta/\mp\theta)_s$, $(\pm\theta/\mp\theta/0_2)_s$, $(90_2/\pm\theta/\mp\theta)_s$, and $(\pm\theta/\mp\theta/90_2)_s$ laminates. Values of θ equal to 30, 45, and 60 degrees were selected. Loading was uniform stress in the 0° direction and a uniform temperature change. The results from the SAP IV three-dimensional finite element model showed that changing the stacking sequence changed the magnitude and sometimes the sign of the midplane interlaminar stress distribution for σ_z around the hole. The sign of σ_z changed for some stacking sequences, but no general rule was apparent for the relationship between the sign of σ_z and the far field stresses. The $(0/90)_s$ and $(90/0)_s$ comparisons for stress loading showed a change in sign of the σ_z stress distribution and also stress change in magnitude. For example, σ_z changed from .25 for the $(90/0)_s$ laminate to .03 for the $(0/90)_s$ laminate at $\theta = 90°$. Based on the results for the $(0_2/\pm\theta/\mp\theta)_s$ and $(90_2/\pm\theta/\mp\theta)_s$, there was a trend for larger values of σ_z to occur in the laminates with the (0_2) and (90_2) plys in the center. The sign of the σ_z distribution for the $(\pm 60/\mp 60/90_2)$ laminate has a sign change at $\theta = 90°$ for a modification of the stacking sequence which places the (90_2) plys on the outside. However, at $\theta = 0$, the sign of σ_z is unchanged for a change in stacking

sequence. The effect of a uniform temperature loading condition coupled with a change in stacking sequence was that the $(\pm 30/\mp 30/90_2)_s$ and $(90_2/\pm 30/\mp 30)_s$ laminates showed a change in the sign of σ_z distributions around the hole. The other two laminates had σ_z distributions that did not change sign around the circular hole. However, the sign and magnitude of these stress distributions changed with stacking sequence.

A study of the effects of lay-up angle in the $(0_2/\pm\theta/\mp\theta)_s$, $(\pm\theta/\mp\theta/0_2)_s$, $(90_2/\pm\theta/\mp\theta)_s$, and $(\pm\theta/\mp\theta/90_2)_s$ laminates for values of θ equal to 30, 45, and 60 degrees was presented. Two types of loading conditions were considered; an applied stress in the 0° direction and a uniform temperature change to represent the fabrication process. The results of the uniform stress loading applied to the $(\pm\theta/\mp\theta/0_2)_s$ and $(\pm\theta/\mp\theta/90_2)_s$ laminates were that the value of σ_z on the edge of the hole at an angle of 90° to the loading increased as the lay-up angle increased from 30 to 60 degrees. Becasue of the constant stress loading conditior and the reduction in compliance of the laminates for increasing values θ, there is a higher applied stress in the 0° ply for increasing θ as shown in Table A-2 This means that the inplane tangential stress in the (0_2) plys and the (90_2) plys at $\theta = 90°$ also increases as θ increases. The maximum tensile value of σ_z increased for increasing values of θ for the $(\pm\theta/\mp\theta/0_2)_s$, $(\pm\theta/\mp\theta90_2)_s$, and $(0_2/\pm\theta/\mp\theta)_s$. The temperature loading condition gave a maximum value of σ_z for the $(90_2/\pm\theta/\mp\theta)_s$ laminate with a lay-up angle of $\theta = 45°$.

The study directed at the effect of residual stresses due to fabrication of the laminate was based on a temperature change of -200 F. Values of the interlaminar stress σ_z from the tensile range of 800 to 1820 psi resulted. Inplane tensile stresses were as high as 9750 psi. This indicated that the residual stresses can be an important factor in predicting the response of laminated composites, particularly failure modes such as dedamination or ply splitting.

A comparison of the LPT stress distributions and those obtained from the three-dimensional finite element model showed that there was not close agreement for the tangential stresses around a circular hole. It cannot be concluded that all laminates would give similar results. The closeness of the LPT and three-dimensional results appears to be related to the difference in Poisson's ratios of the plys. For example, results were obtained (but not shown in this report) for Poisson's ratios of .3 and .5 for adjacent groups of plys indicated close agreement between LPT and three-dimensional tangential

stresses around the circular hole. The comparisons showing the larger differences between LPT and three-dimensional results occurred for Poisson's ratios of .3 and 1.2 for adjacent groups of plys.

The effect of laminate thickness was considered for a particular laminate with stress loading conditions. Ratios of laminate thickness to hole diameter in the range of .45 to 1.80 were considered. For the cases considered, the highest value of tangential stress occurring around the circular hole changed by about 10 percent. The distribution for the interlaminar stress, σ_z, maintained the same shape, but decreased in magnitude as the ratio of laminate thickness to hole diameter decreased. In general, the peak tension or compression stresses at a ratio of laminate thickness to hole diameter of .45 were about 2/3 of the values at a ratio of 1.8.

A comparison of the LPT and three-dimensional finite element results with experimental data was done for one laminate. The comparison showed good agreement between the predicted and measured tangential strain distributions around a circular hole. This provides a degree of confidence in the three-dimensionaal model. While these results indicate that the inplane behavior around the circular hole can be predicted with LPT and are in agreement with the three-dimensional results, it is pointed out that the Poisson's ratios for adjacent plys were close (.3 and .78) and that the study is too short to be generalized for all laminates. For example, while the average strains around a circular hole appeared close to the LPT solution, the strain distribution varied from the 0° plys to the $\pm$ 45° plys as well as within each ply.

The results of this study show that the interlaminar stress distributions around a circular hole have different characteristics than thos of the straight free edge. It appears that the stress concentration and the variation in stress distributions around the circular hole contribute to the complexity of the problem of relating the sign of σ_z to the field stresses. Thus, equilibrium alone may not be sufficient to determine the sign of σ_z. Consideration of other information such as compatability may be needed. For example, in the straight free edge problem, References [6] and [18] showed that the interlaminate stress σ_z between the first and second plys of a four-ply system could not always be predicted from equilibrium. This σ_z stress could be of a different sign than that at the midplane. Similarly, in the study presented here for circular holes, the sign of the interlaminate stress, σ_z, off the midplane, was not always the

same as that at the midplane. This is an important point to make because an understanding of the signs of σ_z is needed if one is to consider a relationship between the magnitude of σ_z and the initiation of the delamination mode of failure.

One important result of a three-dimensional study of the stress distributions around holes in laminated plates is to provide information and results to develop and gain confidence in a simpler model that can be used routinely. As a first step toward accomplishing this, an approximate analysis for a wedge of a laminate was used to estimate the sign of σ_z at selected points. The input to this model is the distribution of stresses around the hole obtained from the LPT solution. Comparisons of results from this model and the three-dimensional finite element results showed agreement in 19 out of the 24 cases examined. Agreement between the approximate analysis and the three-dimensional finite element results occurred at $\theta = 90$ degrees from the applied load. There was agreement in all cases considered at this location. Disagreement occurs between the approximate analysis and the three-dimensional analysis occurred at $\theta = 0°$ from the load direction for 5 out of 12 cases. If the far field stressed would have been used at this location, disagreement would have occurred in 7 our of the 12 cases. While the approximate analysis presented ignores the interlaminar shear stresses in the equilibrium equations, the model can be expended to include these stresses.

In concluding, the three-dimensional finite element models presented here have been selected to address several important questions pertinent to the design and analysis of laminated plates containing a hole. It is emphasized that only a small number of cases were considered here and the conclusions are based on these cases. Within this context, the study does provide insight into the stress behavior around holes in laminated plates and a means for constructing as approximate analysis to evaluate the sign of the interlaminar stress, σ_z.

REFERENCES

[1] Pipes, R. B., Kaminski, B. E., and Pagano, N. J., "Influence of the Free Edge upon the Strength of Angle-Ply Laminates", in Analysis of the Test Methods for High Modulus Fibers and Composites, ASTM STP 521, 1973, pp 218-228.

[2] Foye, R. L. and Baker, D. J., "Design of Orthotropic Laminates", presented at the 11th Annual AIAA Structures, Structural Dynamics and Materials Conference, Denver, Colorado, April, 1970.

[3] Pipes, R. B. and Pagano, N. J., "Interlaminar Stresses in Composites under Uniform Axial Extension", Journal of Composites Materials, Vol. 4, October, 1970, pp 538-548.

[4] Rybicki, E. F., "Approximate Three-Dimensional Solutions for Symmetric Laminates under Inplane Loading", Journal of Composite Materials, Vol. 5, July, 1971, pp 354-360.

[5] Pagano, N. J., "On the Calculation of Interlaminar Normal Stress in Composite Laminates", Journal of Composite Materials, Vol. 8, January, 1974, pp 89-105.

[6] Pagano, N. J. and Rybicki, E. F., "On the Significance of Effective Modulus Solutions for Fibrous Composites", Journal of Composite Materials, Vol. 8, 1974, pp 214-228.

[7] Pagano, N. J. and Pipes, R. B., "The Influence of Stacking Sequence on Laminate Strength", Journal of Composite Materials, Vol. 5, January, 1971, pp 55-57.

[8] Pagano, N. J. and Pipes, R. B., "Some Observations on the Interlaminar Strength of Composite Materials", International Journal of Mechanical Sciences, Vol. 15, 1973, pp 679-688.

[9] Lackman, L. M. and Pagano, N. J., "On the Prevention of Delamination in Composite Laminates", presented at AIAA/ASME/SAE 15th Structures, Structural Dynamics and Materials Conference, Las Vegas, Nevada, April 17-19, 1974, AIAA Paper No. 74-355.

[10] Dana, J. R. and Barker, R. M., "Three-Dimensional Analysis for the Stress Distribution Near Circular Holes in Laminated Composites", Report VPI-E-74-18 from Virginia Polytechnic Institute and State University to Department of Defense, U. S. Army, Contract No. DAA-F07-69-C-0444 with Watervliet Arsenal, Watervliet, New York, August, 1974.

[11] Rybicki, E. F. and Hopper, A. T., "Analytical Investigation of Stress Concentrations Due to Holes in Fiber Reinforced Plastic Laminated Plates, Three-Dimensional Models", Technical Report AFML-TR-73-100, June, 1973.

[12] Daniel, I. M., Rowlands, R. E., and Whiteside, J. B., "Effects of Material and Stacking Sequence on Behavior of Composite Plates with Holes", Experimental Mechanics, Vol. 14, No. 1, January, 1974, pp 1-9.

[13] Greszczuk, L. B., "Stress Concentraions and Failure Criteria for Orthotropic and Anisotropic Composite Plates with Circular Openings", Composite Materials: Testing and Design (Second Conference), ASTM STP 497, 1972.

[14] Waddoups, M. E., Eisenmann, J. R., and Kaminski, B. E., "Macroscopic Fracture Mechanics of Advanced Composite Materials", Journal of Composite Materials, Vol. 5, October, 1971, p 446-454.

[15] Waszczuk, J. P. and Cruse, T. A., "Failure MOde and Strength Predictions of Anisotropic Bolt Bearing Specimens", AIAA Paper No. 71-354, AIAA/ASME 12th Structural Dynamics and Materials Conference, Anaheim, California, April 19-21, 1971.

[16] Whitney, J. M. and Nuismer, R. J., "Stress Fracture Criteria for Laminated Composites containing Stress Concentration", Journal of Composite Materials, Vol., 8, 1974, pp 253-265.

[17] SAP IV, A Structural Analysis Program for Static and Dynamic Response of Linear Systems by Klaus-Jurgen Bathe, Edward L. Wilson, and Fred E. Peterson, Report No. EERC 73-11 from College of Engineering, Univeristy of California at Berkeley to National Science Foundation, April, 1974.

[18] Rybicki, E. F. and Pagano, N. J., "A Study of the Influence of Microstructure on the Modified Effective Modulus Approach for Composite Laminates", Proceedings of the 1975 International Conference on Composite Materials, Published by the Metallurgical Society of AIME, New York, New York, Edited by E. Scala, E. Anderson, I. Toth, and B. Noton, Vol. 2, pp 149-159.

[19] Private Communication with Dr. N. J. Pagano.

[20] Ashlon, J. E., Halpen, J. C., and Petit, P. H., "Primer on Composite Materials Analysis" Technomic Publishing Co., Inc., Stanford, Conn.

[21] Private Communication with Dr. I. M. Daniel.

APPENDIX

PROPERTIES AND RESULTS FOR $(\pm\theta/\mp\theta/0_2)_s$ AND $(\pm\theta/\mp\theta/90_2)_s$ LAY-UPS

APPENDIX

PROPERTIES AND RESULTS FOR $(\pm\theta/\mp\theta/0_2)_s$ AND $(\pm\theta/\mp\theta/90_2)_s$ LAY-UPS

The purpose of this appendix is to present the material properties, stress boundary conditions, and stress distribution for the analyses of $(\pm\theta/\mp\theta/0_2)_s$, $(0_2/\pm\theta/\mp\theta)_s$, $(\pm\theta/\mp\theta/90)_s$, and $(90_2/\pm\theta/\mp\theta)_s$.

For each by-up values of θ equal to 30°, 45° and 60° were considered. Material properties and stress boundary conditions are given in Tables A-1 and A-2 respectively. Results for both mechanical stress and thermal loading conditions are presented in Tables A-3 through A-8 and Tables A-9 through A-11, respectively.

TABLE A-1. MATERIAL PROPERTIES[(a)] FOR $(\pm\theta/\mp\theta/0_2)_s$ LAMINATES

Material Property	Plys			
	0_2°	$(\pm30/\mp30)$	$(\pm45/\mp45)$	$(\pm60/\mp60)$
E_1 (10^6psi)	22.0	8.54	3.44	2.03
E_2 (10^6psi)	1.6	2.03	3.44	8.54
E_3 (10^6psi)	1.6	1.65	1.68	1.65
ν_{12}	.25	1.24	.72	.29
ν_{13}	.25	-.035	.08	.18
ν_{23}	.25	.18	.08	-.035
σ_{12} (10^6psi)	1.0	4.54	5.73	4.54
σ_{13} (10^6psi)	1.0	.88	.78	.70
σ_{23} (10^6psi)	.64	.70	.78	.88
α_1 (10^{-6}/F)	-1.5	-2.99	-.36	6.04
α_2 (10^{-6}/F)	12.4	6.04	-.36	-2.99
α_3 (10^{-6}/F)	12.4	14.36	15.3	14.36

(a) Values obtained from Reference [19].

TABLE A-2. STRESS BOUNDARY CONDITIONS FOR $(\pm\theta/\mp\theta/0_2)_s$ AND $(\pm\theta/\mp\theta/90_2)_s$ LAMINATES TO PRODUCE A UNIT STRESS IN THE 0° OR y DIRECTIONS

Laminate	(0_2°) or (90_2°) Plys			$(\pm\theta/\mp\theta)$ Plys		
	σ_x	σ_y	σ_{xy}	σ_x	σ_y	τ_{xy}
	(psi)			(psi)		
$(\pm30/\mp30/0_2)_s$	-.094	1.612	0.0	.047	.693	0.0
$(\pm45/\mp45/0_2)_s$	-.069	2.243	0.0	.035	.378	0.0
$(\pm60/\mp60/0_2)_s$	-.007	2.531	0.0	.004	.234	0.0
$(\pm30/\mp30/90_2)_s$	-.695	.171	0.0	.348	1.414	0.0
$(\pm45/\mp45/90_2)_s$	-1.431	.350	0.0	.716	1.324	0.0
$(\pm60/\mp60/90_2)_s$	-1.524	1.702	0.0	.7620	1.148	0.0

TABLE A-3. STRESSES AT LAMINATE MIDPLANE FOR $(+30/\bar{+}30/0_2)_s$ AND $(\pm45/\bar{+}45/0_2)_s$ LAY-UPS WITH UNIT STRESS IN THE Y-DIRECTION

		Angle Measured From Y-Axis						
	Stress	0°	13.3°	26.6°	45.0°	63.4°	76.7°	90°
$(\pm30/\bar{+}30/0_2)_s$	σ_x	- .3884	-.3153	-.2138 (-.2019)*	.0078	.09868 (.1319)*	.1709	.0520
	σ_y	- .8774	.4035	.6313 (.2994)	-1.3419	1.5913 (1.7429)	5.0228	7.2951
	σ_z	- .2030	-.1889	-.1715 (-.1746)	- .0741	.0632 (.0743)	.1383	.1485
	τ_{xy}	- .0036	.1083	.1007 (.1252)	- .1059	-.2805 (-.3183)	-.2971	-.0084
	σ_θ	- .3884	-.3258	-.1250 (-.2016)	- .5612	1.5167 (1.6748)	4.8991	7.2951
$(\pm45/\bar{+}45/0_2)_s$	σ_x	- .3896	-.3079	-.2288 (-.2017)	.0331	.1637 (.1987)	.2048	-.0068
	σ_y	-1.2190	.5994	.8513 (.5309)	-1.7864	1.8872 (2.1231)	6.3228	9.3448
	σ_z	- .3448	-.3321	-.3205 (-.3195)	- .1887	.0216 (.0347)	.1467	.1857
	τ_{xy}	- .0056	.1060	.1045 (.1240)	- .1603	-.3893 (-.4287)	-.4084	-.0168
	σ_θ	- .3846	-.3073	-.0959 (-.1541)	- .7164	1.8534 (2.0806)	6.1819	9.3488

* Parentheses denote stresses from adjacent element.

TABLE A-4. STRESSES AT LAMINATE MIDPLANE FOR $(+60/\bar{+}60/0_2)_s$ AND $(+30/\bar{+}30/90_2)_s$ LAY-UPS WITH UNIT STRESS IN THE Y-DIRECTION

		Angle Measured From Y-Axis						
	Stress	0°	13.3°	26.6°	45.0°	63.4°	76.7°	90°
$(\pm 60/\bar{+}60/0_2)_s$	σ_x	- .3030	-.2348	-.1760 (-.1435)(a)	.0892	.2226 (.2562)(a)	.2081	.0685
	σ_y	-1.3052	.6846	.9680 (.6010)	-1.8959	2.1209 (2.4156)	7.0106	10.3716
	σ_z	- .3759	-.3612	-.3518 (-.3503)	- .2339	-.0247 (-.0110)	.1108	.1606
	τ_{xy}	- .0038	.0853	.0736 (.0956)	- .2214	-.4728 (-.5103)	-.4826	-.0238
	σ_θ	- .3030	-.2243	-.0056 (-.0708)	- .6820	2.1189 (2.3913)	6.8667	10.3716
$(\pm 30/\bar{+}30/90_2)_s$	σ_x	-3.2425	2.2652	-.5955 (-.6357)	.7515	-.0871 (-.3034)	-.1482	.4282
	σ_y	.0362	-.0606	.0032 (.0096)	.1727	.4242 (.4187)	.5576	.6312
	σ_z	.0510	.0481	.0991 (.0998)	.2083	.2593 (.2540)	.2588	.2551
	τ_{xy}	.0095	.0932	.0396 (.0322)	-.1029	.1895 (-.1700)	.1434	.0021
	σ_θ	-3.2425	-2.1903	-.5072 (-.5321)	.5650	.4734 (.4101)	.5845	.6312

(a) Parentheses denote stresses from adjacent element.

TABLE A-5. STRESSES AT LAMINATE MIDPLANE FOR $(\pm 45/\mp 45/90_2)_s$ AND $(\pm 60/\mp 60/90_2)_s$ LAY-UPS WITH UNIT STRESS IN THE Y-DIRECTION

		Angle Measured From Y-Axis						
	Stress	0°	13.3°	26.6°	45°	63.4°	76.7°	90°
$(\pm 45/\mp 45/90_2)_s$	σ_x	-5.0802	-3.5907	-1.1046 (-1.0455)[a]	1.2395	.0766 (-.2587)[a]	-.1108	.3889
	σ_y	.0305	-.1071	-.0003 (.0328)	.2484	.7210 (.7079)	1.0251	1.2216
	σ_z	.0249	.0309	.1168 (.1262)	.3468	.5291 (.5198)	.6083	.6593
	τ_{xy}	.0122	.1490	.1122 (.0739)	-.1612	-.3419 (-.3105)	-.2858	.0034
	σ_θ	-5.0802	-3.4731	-.9730 (-.8885)	.9052	.8656 (.7627)	1.0930	1.2216
$(\pm 60/\mp 60/90_2)_s$	σ_x	-5.7912	-4.0572	-1.2263 (-1.0891)	1.5996	.2920 (-.1168)	-.0191	.4340
	σ_y	.0261	-.1343	.0536 (.1067)	.4291	1.1897 (1.1769)	1.6766	1.9957
	σ_z	-.1422	-.1327	-.0202 (-.0044)	.2427	.4953 (.4846)	.6191	.7156
	τ_{xy}	.0188	.1175	.0443 (-.0167)	-.3698	-.5822 (-.5447)	-.4760	.0004
	σ_θ	5.7912	-3.9022	-1.0052 (-.8360)	1.3842	1.4759 (1.3537)	1.801	1.9957

(a) Parentheses denote result from adjacent element.

TABLE A-6. STRESSES AT LAMINATE MIDPLANE FOR $(0_2/\pm30/\mp30)_s$ AND $(0_2/+45/\mp45)_s$ LAY-UPS WITH UNIT STRESS IN THE Y-DIRECTION

		Angle Measured From Y-Axis						
	Stress	0°	13.3°	26.6°	45.0°	63.4°	76.7°	90.0°
$(0_2/\pm30/\mp30)_s$	σ_x	-.3630	-.3663	-.1756 (-.1892)[a]	.1207	.3389 (.3836)[a]	.3085	.0348
	σ_y	.0794	-.2065	-.0056 (-.0132)	.4787	1.5028 (1.5762)	2.2063	2.4048
	σ_z	.0681	.0653	-.0635 (.0615)	.0380	.0068 (.0129)	-.0289	-.0812
	τ_{xy}	-.0235	.2608	.0793 (.0818)	-.3261	-.6469 (-.7504)	-.7908	-.0206
	σ_θ	-.3630	-.4746	-.2050 (-.2194)	.6258	1.7874 (1.9380)	2.2895	2.4048
$(0_2/\pm45/\mp45)_s$	σ_x	-.5922	-.5804	-.1927 (-.2328)	.2955	.3457 (-.3866)	.2023	.0107
	σ_y	-.0071	-.1881	.0486 (.0436)	.5962	.9476 (.9712)	1.0209	.9826
	σ_z	.1810	.1643	.1446 (.1428)	.0938	.0106 (.0131)	-.0364	-.0610
	τ_{xy}	-.0550	.3323	.0412 (-.0084)	-.4450	-.5445 (-.6183)	-.4900	-.0023
	σ_θ	-.5922	-.7084	-.1773 (-.1841)	.8909	1.2629 (1.3491)	1.197	0.9826

(a) Parentheses denote result from adjacent element.

TABLE A-7. STRESSES AT LAMINATE MIDPLANE FOR $(0_2/\bar{\pm}60/\pm60)_s$ AND $(90_2/\pm30/\bar{\pm}30)_s$ LAY-UPS WITH UNIT STRESS IN THE Y-DIRECTION

		Angle Measure From Y-Axis						
	Stress	0°	13.3°	26.6°	14.0°	63.4°	76.7°	90.0°
$(0_2/\pm60/\bar{\pm}60)_s$	σ_x	-1.1902	-.9025	-.1906 (-.2140)(a)	.4736	.2272 (.2787)(a)	.0807	.0377
	σ_y	-.0426	-.0994	.0823 (.0898)	.4296	.5591 (.5833)	.5897	.5980
	σ_z	.2328	.2049	.1689 (.1702)	.1151	.0235 (.0268)	- .0202	-.0358
	τ_{xy}	.0395	.2277	-.0092 (-.0640)	-.4014	-.4098 (-.4423)	- .2496	-.0351
	σ_θ	1.1902	-.9620	-.1285 (-.1018)	.8530	.8207 (.8764)	.6745	.5980
$(90_2/\pm30/\bar{\pm}30)_s$	σ_x	.1551	-.1960	.0785 (.0577)	.4667	.6163 (.6697)	.4747	.1083
	σ_y	.2324	-.3028	.0899 (.0710)	1.1090	2.5297 (2.6066)	3.3611	3.6397
	σ_z	-.1137	-.1201	-.1003 (-.1033)	-.1016	-.1026 (-.0952)	-.1350	-.1898
	τ_{xy}	-.0282	.3029	-.0973 (-.0881)	-.7736	-1.1101 (-1.2450)	-1.1709	-.0341
	σ_θ	-.1551	-.3373	.1587 (.1309)	1.5615	3.0350 (3.2152)	3.7326	3.6397

(a) Parentheses denote result from adjacent element.

TABLE A-8. STRESSES AT LAMINATE MIDPLANE FOR $(90_2/+45/\bar{+}45)_s$ AND $(90_2/+60/\bar{+}60)_s$ LAY-UPS WITH UNIT STRESS IN THE Y-DIRECTION

		Angle Measure From Y-Axis						
	Stress	0°	13.3°	26.6°	45.0°	63.4°	76.7°	90°
$(90_2/\pm45/\bar{+}45)_s$	σ_x	-.2646	-.3277	.4439 (.3949)[a]	1.3057	.8858 (.9352)[a]	.3711	.1748
	σ_y	.1305	-.2867	.3891 (.3791)	1.8047	2.3050 (2.3139)	2.2213	2.2123
	σ_z	-.1351	-.1644	-.1447 (-.1470)	-.1669	-.2493 (-.2471)	-.3164	-.3315
	τ_{xy}	-.0738	.3861	-.4511 (-.5016)	-1.4806	-1.2686 (-1.3888)	-.8193	-.0666
	σ_θ	-.2646	-.4984	.7941 (.7931)	3.0358	3.0363 (3.1495)	2.4902	2.2123
$(90_2/\pm60/\bar{+}60)_s$	σ_x	1.1889	-.7547	.6513 (.6621)	1.8387	.6902 (.7709)	.1723	.3296
	σ_y	-.0011	-.0980	.4901 (.5188)	1.5444	1.9020 (1.9176)	1.9358	2.0243
	σ_z	-.0657	-.1123	-.1074 (-.1032)	-.1131	-.1977 (-.1960)	-.2584	-.2616
	τ_{xy}	-.0291	.0745	-.6199 (-.7244)	-.4912	-1.1246 (-1.1804)	-.5169	-.0911
	σ_θ	-1.1889	-.7533	1.1154 (1.2134)	3.1828	2.5596 (2.6329)	1.9582	2.0243

(a) Parentheses denote result from adjacent element.

TABLE A-9. STRESSES AT LAMINATE MIDPLANE FOR $(\pm 30/\mp 30/90_2)_s$ AND $(90_2/\pm 30/\mp 30)_s$ LAY-UPS WITH THERMAL LOADING OF $\Delta T = -200°F$

		Angle Measured From Y-Axis						
	Stress	0°	13.3°	26.6°	45°	63.4°	76.7°	90°
$(\pm 30/\mp 30/90_2)_s$	σ_x	-11563.5	-7795.4	-1494.7 (-1206.6)[a]	4710.5	320.7 (177.2)[a]	- 230.1	481.7
	σ_y	- 127.1	-1093.3	- 112.3 (78.4)	1278.1	3794.3 (4158.5)	5167.6	6121.6
	σ_z	- 3295.8	-2944.0	-1911.6 (-1858.6)	- 653.6	722.1 (810.5)	1366.1	1815.1
	τ_{xy}	187.6	34.8	- 465.1 (-685.3)	-1769.3	-1766.2 (-1850.7)	-1483.4	12.4
	σ_θ	-11563.5	-7425.1	(-845.1) (-400.2)	4763.6	4512.1 (4842.2)	5546.1	6121.6
$(90_2/\pm 30/\mp 30)_s$	σ_x	3447.1	3432.9	3248.0 (3055.0)	2003.9	263.2 (-16.8)	- 672.9	217.8
	σ_y	- 65.5	450.8	828.3 (503.8)	1109.4	-2191.8 (-2766.8)	-5466.8	-6207.1
	σ_z	834.2	873.7	722.7 (696.2)	93.9	- 598.7 (- 636.4)	-1009.1	- 999.6
	τ_{xy}	- 64.25	-1143.7	-1572.4 (-1376.3)	-1348.7	27.2 (544.8)	1594.5	62.4
	σ_θ	3447.1	3787.1	4022.0 (3645.5)	2905.3	-1721.3 (-2659.6)	-5927.1	-6207.1

(a) Parentheses denote result from adjacent element.

TABLE A-10. STRESSES AT LAMINATE MIDPLANE FOR $(\pm 45/\mp 45/90_2)_s$ AND $(90_2/\pm 45/\mp 45)_s$ LAY-UPS WITH THERMAL LOADING OF $\Delta T = -200°F$.

		Angle Measured From Y-Axis						
	Stress	0°	13.3°	26.6°	45°	63.4°	76.7°	90°
$(\pm 45/\mp 45/90_2)_s$	σ_x	- .248	- 54.1	1192.9 (748.0)[a]	-1869.3	594.2 (630.7)[a]	382.9	297.9
	σ_y	- 248.1	726.2	154.1 (266.3)	1153.3	2979.4 (3254.5)	3931.4	4575.0
	σ_z	-3005.5	-2819.4	-2157.9 (-2137.9)	-1653.1	- 874.0 (-1515.3)	- 596.1	- 368.1
	τ_{xy}	124.2	- 550.7	- 997.0 (-1130.8)	1786.1	-1439.4 (-1515.3)	-1138.7	2.4
	σ_θ	- .248	156.9	1782.9 (1556.8)	3297.4	3653.7 3941.8)	4253.4	4575.0
$(90_2/\pm 45/\mp 45)_s$	σ_x	640.1	720.6	88.8 (8.47)	- 875.9	- 620.0 (- 796.9)	- 339.1	76.7
	σ_y	-243.7	241.3	- 310.2 (- 418.7)	-1634.4	-2099.9 (-2281.6)	-2123.7	-1942.5
	σ_z	1017.5	1067.4	941.0 (932.9)	702.8	474.4 (460.4)	395.1	375.7
	τ_{xy}	84.5	- 516.8	267.1 (408.3)	1128.2	966.3 (1160.7)	767.5	64.5
	σ_θ	640.1	926.6	- 205.1 (- 417.6)	-3638.5	-2576.9 (-2913.3)	-2372.9	-1942.5

(a). Parentheses denote result from adjacent element.

TABLE A-11. STRESSES AT MIDPLANE FOR $(\pm 60/\mp 60/90_2)_s$ AND $(90_2/\pm 60/\mp 60)_s$ LAY-UPS WITH THERMAL LOADINGS OF ΔT = 200 F

	Stress	0°	13.3°	26.6°	45°	63.4°	76.7°	90°
$(\pm 60/\mp 60/90_2)_s$	σ_x	9573.7	6256.5	2903.5 (2073.1)[a]	-1098.3	567.6 (715.1)[a]	606.1	- 537.3
	σ_y	- 206.1	- 210.4	283.2 (300.2)	652.1	1366.1 (1484.8)	1701.9	1907.9
	σ_z	-1638.1	1661.4	-1508.7 (-1519.6)	-1703.5	-1598.2 (-1565.9)	-1643.8	-1644.3
	τ_{xy}	43.6	- 769.3	-1065.7 (-1090.3)	-1191.8	- 684.1 (- 727.8)	- 493.8	- .4855
	σ_ξ	9573.7	6258.9	3231.5 (2590.6)	968.7	1753.7 (1913.2)	1865.1	1907.9
$(90_2/\pm 60/\mp 60)_s$	σ_x	-2740.5	-2764.9	-2585.6 (-2574.5)	-1661.8	-319.8 (-331.1)	184.1	-367.9
	σ_y	- 62.9	- 408.6	- 767.2 (- 746.9)	- 938.4	-676.7 (-681.5)	- 460.2	-525.7
	σ_z	732.4	741.5	730.7 (733.7)	818.2	886.1 (885.4)	960.1	952.2
	τ_{xy}	62.9	984.1	1268.3 (1198.2)	1114.6	450.4 (457.6)	- 136.8	45.8
	σ_θ	-2740.5	-3080.8	-3236.5 (-3167.5)	2414.7	- 965.7 (- 977.6)	- 364.8	-525.7

(a) Parentheses denote result from adjacent element.

TABLE A-12. THREE-DIMENSIONAL FINITE ELEMENT RESULTS[(a)] AND LPT SOLUTIONS FOR TANGENTIAL STRESS DISTRIBUTIONS FOR $(0_2/\pm30/\mp30)_s$, $(\pm30/\mp30/0_2)_s$, $(0_2/\pm45/\mp45)_s$, AND $(\pm45/\mp45/0_2)_s$ LAMINATES

	$(\pm30/\mp30/0_2)_s$ (0_2) Plys		$(0_2/\pm30/\mp30)_s$ (∓30) Plys	
θ	Three-Dimensional Analysis	LPT	Three-Dimensional Analysis	LPT
0°	-.3884	-.2835	-.3630	-.4637
13.3°	-.3258	-.2242	-.4746	-.4646
26.6°	-.1250	-.1026	-.2050	-.3892
45.0°	-.5612	.0815	.6258	.3384
63.4°	1.5167	1.7981	1.7874	2.1158
76.7°	4.8991	4.5609	2.2896	2.6173
90.0°	7.2951	5.8391	2.4048	2.5129

	$(\pm45/\mp45.0_2)_s$ (0_2) Plys		$(0_2/\pm45/\mp45)_s$ (∓45) Plys	
θ	Three-Dimensional Analysis	LPT	Three-Dimensional Analysis	LPT
0°	-.3846	-.2317	-.5922	-.8749
13.3°	-.3073	-.1631	-.7034	-.8251
26.6°	-.0959	-.0551	-.1773	-.5195
45.0°	-.7164	.2739	.8909	.9065
63.4°	1.8534	3.0262	1.2629	2.0203
76.7°	6.1819	5.6950	1.197	1.5066
90.0°	9.3488	6.7456	.9826	1.1379

(a) Evaluated at laminate midplane.

TABLE A-13. THREE-DIMENSIONAL FINITE ELEMENT RESULTS[(a)] AND LPT SOLUTIONS FOR TANGENTIAL STRESS DISTRIBUTIONS FOR $(\pm 60/\mp 60/0_2)_s$, $(0_2/\pm 60/\mp 60)_s$, $(\pm 30/\mp 30/90_2)_s$, AND $(90_2/\pm 30/\mp 30)_s$ LAMINATES

	$(\pm 60/\mp 60/0_2)_s$ (0_2) Plys		$(0_2/\pm 60/\mp 60)_s$ (∓ 60) Plys	
θ°	Three-Dimensional Analysis	LPT	Three-Dimensional Analysis	LPT
0°		-.1715	-1.1902	-1.4142
13.3°		-.1226	- .9620	-1.1211
26.6°	-.0056	-.0384	- .1285	- .2778
45.0°	-.6820	.6484	.8530	1.1756
63.4	2.1189	3.5333	.8207	1.5303
76.7	6.8667	6.3164	.6745	1.0242
90°	10.3716	7.5932	.5980	.7033

	$(\pm 30/\mp 30/90_2)_s$ (90_2) Plys		$(90_2/\pm 30/\mp 30)_s$ (∓ 30) Plys	
θ	Three-Dimensional Analysis	LPT	Three-Dimensional Analysis	LPT
0°	-3.2425	-2.5310	-.1551	-.2344
13.3°	-2.1903	-1.7857	-.3373	-.2895
26.6°	- .5072	- .3183	.1587	-.1378
45.0°	.5650	.6486	1.5615	1.1756
63.4°	.4734	.4266	3.0350	3.0837
76.7°	.5845	.4338	3.7326	3.9655
90°	.6312	.5142	3.6397	4.2426

(a) Evaluated at laminate midplane.

TABLE A-14. THREE-DIMENSIONAL FINITE ELEMENT RESULTS[a] AND LPT SOLUTIONS FOR TANGENTIAL STRESS DISTRIBUTIONS FOR $(\pm45/\mp45/90_2)_s$, $(90_2/\pm45/\mp45)_s$, $(\pm60/\mp60/90_2)_s$ AND $(90_2/\pm60/\mp60)_s$ LAMINATES

	$(\pm45/\mp45/90_2)_s$ (90_2) Plys		$(90_2/\pm45/\mp45)_s$ (∓45) Plys	
θ	Three-Dimensional Analysis	LPT	Three-Dimensional Analysis	LPT
0°	-5.0800	-3.3959	- .2646	- .5728
13.3°	-3.4731	-2.3695	- .4984	- .6268
26.6°	- .9730	- .2040	.7941	- .1362
45.0°	.9052	.7001	3.0358	2.3171
63.4°	.8656	.3590	3.0363	3.3851
76.7°	1.0930	.6357	2.4902	3.2162
90°	1.2216	.8158	2.2123	3.0808

	$(\pm60/\mp60/90_2)_s$ (90_2) Plys		$(90_2(\pm60/\mp60)_s$ (∓60) Plys	
θ	Three-Dimensional Analysis	LPT	Three-Dimensional Analysis	LPT
0°	-5.7912	-3.9941	-1.1889	- 1.7187
13.3°	-3.9022	-2.3192	- .7533	- .13309
26.6°	-1.0050	.4136	1.1154	.4867
45.0°	1.3842	.7232	3.1828	3.0020
63.4°	1.4759	.7859	2.5596	2.9797
76.7°	1.8010	1.2314	1.9582	2.5517
90°	1.9957	1.4457	2.0243	2.3647

(a) Evaluated at laminate midplane.

☆ U. S. GOVERNMENT PRINTING OFFICE: 1976 — 757-001/37